

The genetic basis of parental care evolution in monogamous mice

Andres Bendesky^{1,2,3}, Young-Mi Kwon^{1,2}, Jean-Marc Lassance^{1,2,3}, Caitlin L. Lewarch^{1,3}, Shenqin Yao^{1,3†}, Brant K. Peterson^{1,2‡}, Meng Xiao He⁴, Catherine Dulac^{1,3,5} & Hopi E. Hoekstra^{1,2,3,4,5,6}

Parental care is essential for the survival of mammals, yet the mechanisms underlying its evolution remain largely unknown. Here we show that two sister species of mice, *Peromyscus polionotus* and *Peromyscus maniculatus*, have large and heritable differences in parental behaviour. Using quantitative genetics, we identify 12 genomic regions that affect parental care, 8 of which have sex-specific effects, suggesting that parental care can evolve independently in males and females. Furthermore, some regions affect parental care broadly, whereas others affect specific behaviours, such as nest building. Of the genes linked to differences in nest-building behaviour, vasopressin is differentially expressed in the hypothalamus of the two species, with increased levels associated with less nest building. Using pharmacology in *Peromyscus* and chemogenetics in *Mus*, we show that vasopressin inhibits nest building but not other parental behaviours. Together, our results indicate that variation in an ancient neuropeptide contributes to interspecific differences in parental care.

In mammals, parental care is critical for the survival of young. Parental behaviour, however, is not uniform and instead varies in form and magnitude among individuals, between sexes, and across species. A particularly variable feature of parental behaviour is the care for young by their fathers, which occurs more often and to a larger extent in monogamous species than promiscuous ones¹.

Parental care, performed by mothers and some fathers, encompasses an array of behaviours including retrieving, huddling, nursing, and grooming pups along with building a nest, which is often initiated or enhanced by the birth of a litter. The rich diversity of parental behaviours raises several questions about the evolution of parental care, particularly in monogamous mammals: how does the genetic architecture differ between males and females? Does evolution act on genetic loci that affect multiple components of parental behaviour in concert or do particular components have independent genetic underpinnings? What specific genes are involved? How does variation in these genes act within neuronal circuits to alter behaviour?

Comparative analyses of species with divergent social systems have offered important insights into the genetic and neurobiological basis of natural variation in social behaviour. Studies of monogamous and promiscuous voles defined a prominent role for the vasopressin and oxytocin pathways in affiliative behaviours, showing, for example, that differences in the spatial distribution of the vasopressin 1a receptor in the male brain are associated with changes in pair-bonding behaviour^{2,3}. Oxytocin and vasopressin are known to regulate many aspects of parental care^{4–7}, but how genetic variation in these pathways contributes to natural differences in parental care is poorly understood.

To study the genetic basis of parental care, we focused on mice of the genus *Peromyscus*, in which both social and genetic monogamy has evolved independently at least twice⁸ (Fig. 1a). One of these lineages consists of the promiscuous deer mouse (*P. maniculatus bairdii*)^{9,10} and its sister species, the monogamous old-field mouse (*P. polionotus*

subgriseus)^{11,12} (Fig. 1a, b). These species are at opposite ends of a monogamy–promiscuity spectrum¹³, yet—in contrast to the classic vole species—they can interbreed in the laboratory. The remarkable divergence in behaviour between such closely related species offers a unique opportunity to define the genomic architecture of a mammalian social behaviour and to identify pathways and genes that contribute to the evolution of parental behaviour.

Monogamous *Peromyscus* are more parental

First, we measured components of both maternal and paternal behaviour (Supplementary Videos 1–8) and found that, in general, *P. polionotus* fathers provided care similar to mothers, whereas *P. maniculatus* fathers provided little parental care. Specifically, *P. polionotus* fathers built nests, licked pups, and huddled pups to the same extent as *P. polionotus* mothers and to a larger extent than both *P. maniculatus* fathers and mothers, but retrieved fewer pups than *P. polionotus* mothers (Fig. 1c–f). *P. maniculatus* fathers did as little nest building and pup licking as *P. maniculatus* mothers but huddled and retrieved pups significantly less than *P. maniculatus* mothers (Fig. 1c–f). Mothers of the two species also differed: *P. polionotus* provided more care than *P. maniculatus* in all behaviours but pup retrieval (Fig. 1c–f). Overall, we observed large differences in parental behaviour, and the differences were most pronounced in fathers.

To test whether these interspecific and between-sex differences in parental behaviour persisted in less-controlled conditions, we videotaped parents in their home cage for 3 consecutive days starting at the birth of a litter. Results were consistent with the shorter behavioural assays: *P. polionotus* fathers were more paternal than *P. maniculatus* fathers, whereas mothers of the two species were similar in their parental care (Extended Data Fig. 1). Together, both the acute and multi-day behavioural patterns aligned with the highly divergent mating systems of these two species.

¹Howard Hughes Medical Institute, Harvard University, Cambridge, Massachusetts 02138, USA. ²Department of Organismic and Evolutionary Biology, Harvard University, Cambridge, Massachusetts 02138, USA. ³Department of Molecular and Cellular Biology, Harvard University, Cambridge, Massachusetts 02138, USA. ⁴Graduate Program in Biophysics, Harvard University, Cambridge, Massachusetts 02138, USA. ⁵Center for Brain Science, Harvard University, Cambridge, Massachusetts 02138, USA. ⁶Museum of Comparative Zoology, Harvard University, Cambridge, Massachusetts 02138, USA. †Present addresses: Allen Institute for Brain Science, Seattle, Washington 98103, USA (S.Y.); Novartis Institutes for BioMedical Research, Cambridge, Massachusetts 02139, USA (B.K.P.).

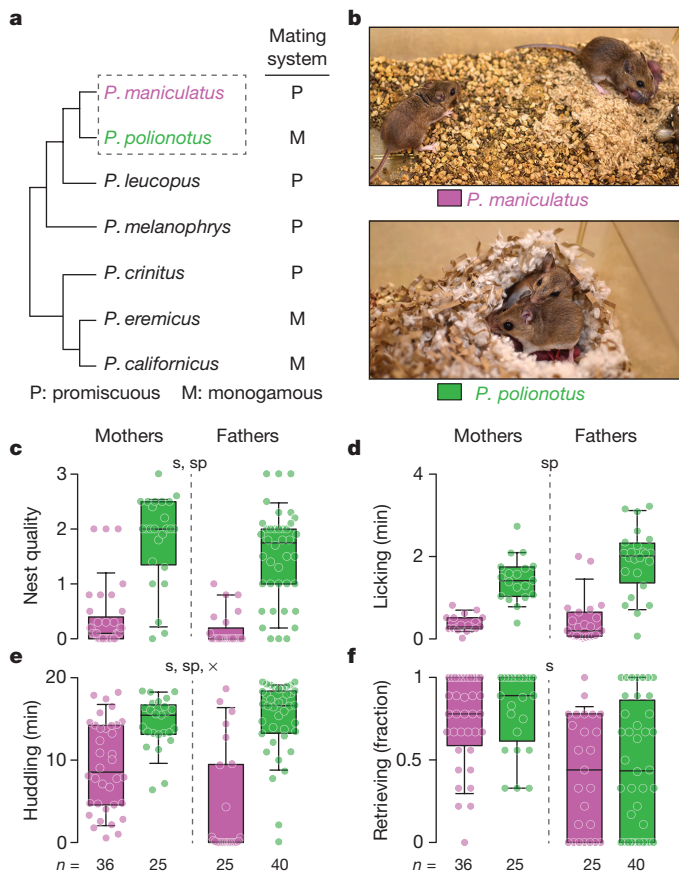


Figure 1 | Parental behaviours of monogamous and promiscuous *Peromyscus* mice. **a**, Cladogram of selected *Peromyscus* species, including known monogamous species (adapted from ref. 8). **b**, Typical *P. maniculatus* and *P. polionotus* parents in the laboratory. **c–f**, Parental behaviours of *P. maniculatus* and *P. polionotus*. Each circle represents the median behaviour of an animal tested three times (**c–e**) or the fraction of pups retrieved over the three tests (**f**). Box plots indicate median, interquartile range, and 10th–90th percentiles. Kruskal–Wallis followed by Dunn’s test (**c**) and two-way analysis of variance (ANOVA) results (**d–f**): significant effects of species (sp), sex (s), or sex-by-species interaction (x) at $P < 0.01$.

Parental behaviour in *Peromyscus* is heritable

To determine whether interspecific differences in parental behaviour are influenced by the parental care received as pups, we cross-fostered *P. polionotus* and *P. maniculatus* pups with parents from the other species (Fig. 2a). The parental behaviour of cross-fostered animals, once they became parents themselves, was indistinguishable from the parental care of non-cross-fostered animals (Fig. 2b–e). There were two exceptions: *P. maniculatus* males raised by *P. polionotus* parents licked and retrieved their own pups less than *P. maniculatus* males raised by their own parents. In summary, the care that pups receive does not explain species differences that emerge in adulthood, consistent with a strong heritable component to parental behaviour.

Differences in parental care also may occur because *P. polionotus* pups demand more care than *P. maniculatus* pups. To test this possibility, we compared the parental behaviour of animals towards their own pups with the behaviour towards pups from the other species. In general, fathers and mothers of both species behaved indistinguishably towards their own pups and pups of the other species (Extended Data Fig. 2 and Supplementary Discussion), indicating that the higher levels of parental behaviour in *P. polionotus* are not due simply to an increased demand for care by their pups.

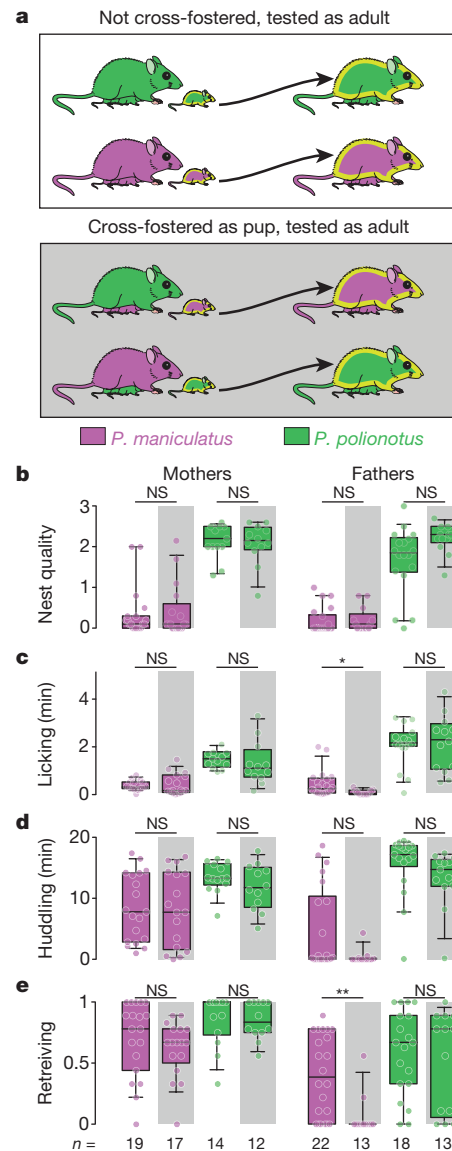


Figure 2 | Effect of cross-fostering on parental behaviour. **a**, Design of the cross-fostering experiment between *P. maniculatus* and *P. polionotus*. **b–e**, Parental behaviour of animals raised by their own parents (white) or by parents of the other *Peromyscus* species (grey). Each circle represents the median behaviour of an animal tested three times. Box plots indicate median, interquartile range, and 10th–90th percentiles. * $P < 0.05$; ** $P < 0.01$; NS, not significant by two-sided Mann–Whitney U -test with Bonferroni correction.

Genetic architecture of parental care

Encouraged by the large and plausibly heritable differences in parental behaviour between *P. polionotus* and *P. maniculatus*, we conducted an interspecies cross to identify genetic components that modulate parental behaviour. We first crossed *P. maniculatus* females to *P. polionotus* males to generate (F_1) hybrids. Next, we intercrossed these F_1 hybrids to generate 769 F_2 hybrids (419 males and 350 females) and measured parental behaviour towards their F_3 pups (Fig. 3a). The distribution of each component of parental care among the F_2 mice encompassed the distributions of both species (Fig. 3b–e). On the basis of the largely unimodal distributions of parental behaviours among the F_2 hybrids, which resembled *P. maniculatus* more closely than *P. polionotus*, the more extensive parental care of *P. polionotus* probably involves more than one genetic locus.

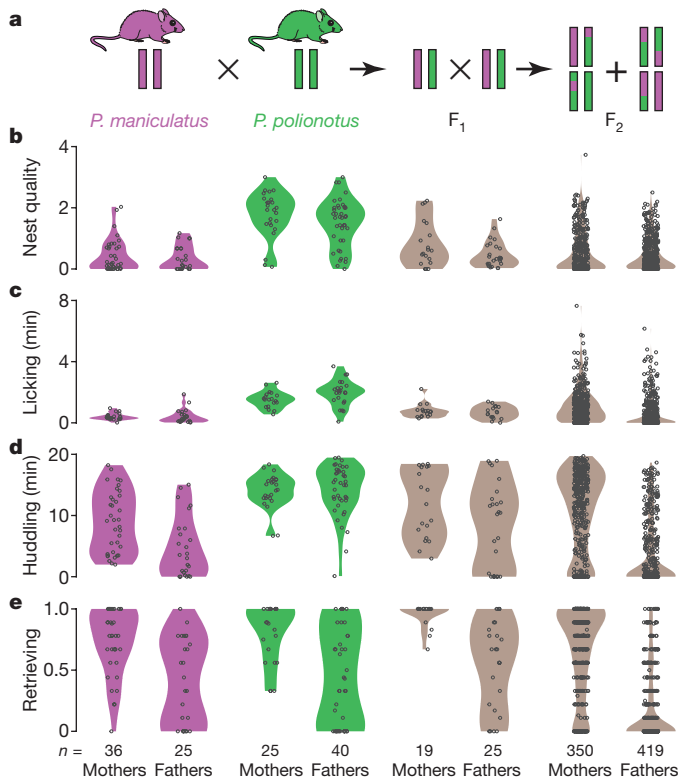


Figure 3 | Distribution of parental behaviours in each species and their interspecific hybrids. **a**, Genetic cross design. Female *P. maniculatus* were mated to *P. polionotus* males to found the cross (see Methods); the behaviour of females and males of each species is shown here for comparison. **b–e**, Violin plots show the distribution of behaviours. Each dot represents the mean behaviour of an animal over three trials.

Next, we tested for correlations among behaviours in the F_2 progeny and analysed the sexes independently (Fig. 4a). We found that times spent huddling and licking were positively correlated in both males and females (Spearman's correlation (r_s) = 0.88, 0.66, respectively), and these two behaviours were also strongly correlated with pup retrieval (huddling–retrieving r_s = 0.60 in males, 0.51 in females; licking–retrieving r_s = 0.52 in males, 0.45 in females). In males, huddling and licking were also correlated with how soon they handled the pup after the assay started (r_s = 0.72 for both). By contrast, in both males and females, nest-building behaviour had much weaker correlations with the other parental behaviours (r_s ranged from 0.23 to 0.43 in males, from 0.22 to 0.31 in females). These results suggest that some genetic loci affect multiple parental behaviours, whereas nest building is more genetically independent from the other behaviours measured.

To identify specific genetic regions that mediate the differences in parental behaviour between *P. polionotus* and *P. maniculatus*, we performed quantitative trait locus (QTL) analysis. To start, we assembled the *P. maniculatus* genome into chromosomes. To genotype the F_2 animals, we combined double-digest restriction-site-associated DNA sequencing (ddRAD-seq¹⁴) with multiplexed shotgun genotyping (MSG¹⁵). Using this strategy, we genotyped the 769 F_2 mice at 406,611 loci and then used the 56,068 most informative loci. By combining behavioural and genetic data, we identified 12 independent QTLs on 11 chromosomes that contribute to 1 or more of the 6 behaviours measured (Fig. 4b and Extended Data Figs 3 and 4; see Supplementary Discussion for validation and potential false positives).

Sex-specific genetics of parental care

Of the 12 QTLs, 8 showed evidence of having different effects in the two sexes as determined by a QTL analysis with sex as a covariate (Fig. 4b). Genotypes at some QTLs preferentially affected the behaviour of one sex, and at other QTLs they affected behaviour in opposite

directions in the two sexes (Extended Data Fig. 4 and Supplementary Discussion). In addition, the strength of correlation between genotype and parental behaviour was often very different between the sexes (Fig. 4b), suggesting that some genetic variants have a stronger effect in one sex than the other. Together, these results indicate that the genetic architecture of parental behaviour differs between males and females.

Several QTLs had effects on specific parental behaviours, whereas others affected more than one behaviour. For example, one QTL on chromosome 4 and one on chromosome 9 were linked to nest building in both males and females, but were not associated with any other behaviours (Fig. 4b, Extended Data Fig. 3 and Supplementary Discussion), consistent with the low phenotypic correlation between nest building and the other parental behaviours (Fig. 4a). By contrast, we found two QTLs that affected several aspects of paternal behaviour: a chromosome 12 QTL affected huddling, licking, and retrieving of pups, and a chromosome 5 QTL affected huddling and latency to handle pups (Fig. 4b and Extended Data Fig. 3). These data raise the possibility that there are genes that have specific behavioural effects and others that can affect parental behaviour more broadly.

A QTL for parental nest building

We next focused on a QTL on chromosome 4 that was associated with parental nest building and had the strongest effect on behaviour of all QTLs (Extended Data Fig. 4). Nest building is a core component of the parental behaviour of vertebrates¹⁶, which, in *Peromyscus*, increases significantly when animals become parents (Extended Data Fig. 5a). Moreover, monogamous *P. polionotus* build more elaborate nests than promiscuous *P. maniculatus* during an acute parental assay, and *P. polionotus* pairs maintain more elaborate nests than *P. maniculatus* for at least 2 weeks after the birth of their pups (Extended Data Fig. 5b). The chromosome 4 QTL was not detected when the nest building of the same animals was measured before mating (data not shown), implying that this QTL is important in a parental context. These results indicate that the chromosome 4 QTL affects an interspecific difference in nesting behaviour that is enhanced by, and maintained during, parenthood.

To identify genes mediating interspecific differences in parental nest building, we first determined which of the genes in the chromosome 4 QTL differed in their protein sequence. Of the 498 genes encompassed by both the male and female QTL regions, 34 had interspecific differences (Supplementary Data File 1), but only 4 were predicted to affect protein function (absolute PROVEAN¹⁷ score > 2.5): sulfide quinone reductase-like and mitochondrial antiviral signalling protein, which localize to mitochondria^{18,19}; congenital dyserythropoietic anaemia type I, which is expressed ubiquitously and involved in erythropoiesis²⁰; and glial cell line-derived neurotrophic factor family receptor alpha-4, a protein not expressed in the brain²¹. None were strong candidates for affecting nest building.

We next determined which of the genes in the QTL differed in expression level between species. We focused on the hypothalamus, a brain area that contains both the medial preoptic area and the paraventricular nucleus (PVN), regions critical for parental nest building in rodents^{22,23}. Only 23 genes differed in expression between the two species (Extended Data Figs 6 and 7a). Of these, nine showed allele-specific expression differences in F_1 hybrids, which provides evidence of local *cis*-acting mutation(s) that affect expression, a feature expected of causal genes in QTL regions (Fig. 5a, Extended Data Fig. 7b and Methods), thereby further narrowing the list of candidate genes.

Vasopressin inhibits nest building

The gene for arginine vasopressin (*Avp*), an important modulator of social behaviours, including maternal care^{5,24}, stood out as a top candidate for variation in nest building. It is found within the large-effect nest-building QTL, highly expressed (among the 4% most highly expressed genes in the hypothalamus), robustly differentially expressed between the two species in both sexes (2.8-fold higher levels in

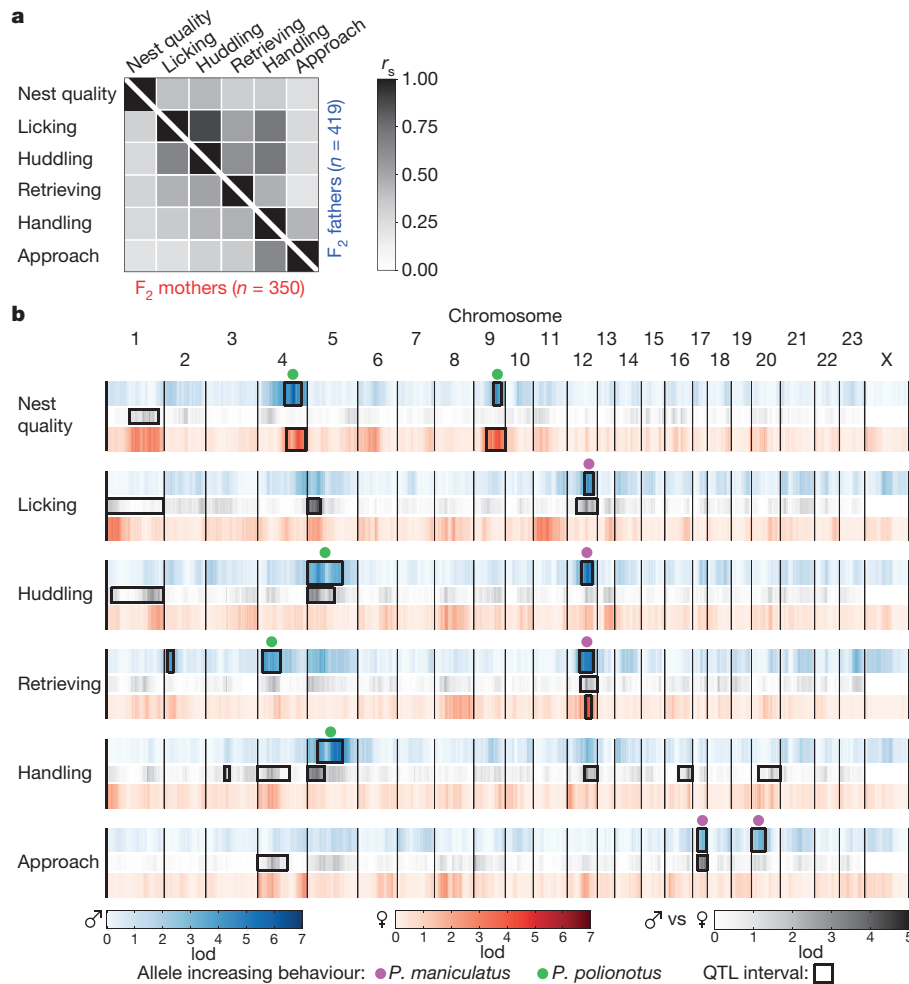


Figure 4 | The genetic architecture of parental behaviour. **a**, Correlation matrix of parental behaviours in F_2 hybrids. **b**, The linkage (lod score) of each behaviour to each marker in each sex and the sex-by-genotype interaction (grey). Boxes delineate the Bayes 0.95 credible interval of QTL of genome-wide significance ($\alpha = 0.05$). Dots denote the allele at

the peak of the QTL that correlates with a higher value for that behaviour (for handling and approach, a decrease in latency to perform behaviour). Heterozygotes at QTLs on chromosomes 2 and 12 (females only) retrieve more pups (see Extended Data Fig. 4 and Supplementary Discussion).

P. maniculatus than *P. polionotus*; moderated *t*-statistic, false discovery rate (FDR)-adjusted $P = 5 \times 10^{-5}$, and showed allele-specific expression (Fig. 5a and Extended Data Figs 7b and 8). These results are consistent with differences in vasopressin protein levels in the PVN of these species²⁵. Moreover, while vasopressin is known to promote anxiety in rodents²⁶, our genetic analyses of anxiety-related behaviour in the same animals argue that effects of vasopressin on parental nest-building behaviour in *Peromyscus* are not mediated simply through changes in anxiety (Extended Data Fig. 9 and Supplementary Discussion). Thus, vasopressin emerged as a strong candidate to test for a role in variation in parental nest-building behaviour in *Peromyscus*.

We next performed pharmacological experiments to determine whether vasopressin regulates nest building in *Peromyscus*. Consistent with the inverse relationship between vasopressin levels and nest building in both *Mus musculus*²⁷ and *Peromyscus* (this study), intracerebroventricular administration of vasopressin into parents of the high nest-building *P. polionotus* inhibited nest building (Fig. 5c). The inhibition of nest building was specific to vasopressin, as the highly similar nonapeptide oxytocin did not have a measurable effect on this behaviour. Remarkably, vasopressin administration did not affect any other parental behaviours measured, in line with the specificity of the QTL containing the vasopressin gene for nest building (Fig. 5c).

To confirm that vasopressin can suppress nest building, we performed chemogenetic experiments in *M. musculus*, where we could specifically manipulate the activity of vasopressin neurons. Consistent

with our expectations, inhibition of vasopressin neurons in the PVN, the only vasopressin nucleus previously implicated in nest building (by lesion studies²³), increased nest building, whereas excitation decreased it (Extended Data Fig. 10 and Supplementary Discussion). Together, our results indicate that vasopressin has an inhibitory effect on parental nest-building behaviour as shown in *P. polionotus* and confirmed in *M. musculus*.

Discussion

Here, using a pair of sister species that lie at opposite ends of the monogamy–promiscuity spectrum, we documented large, heritable differences in parental behaviour and then dissected the genetic architecture of this behavioural variation. Consistent with the largely polygenic nature of variation in behaviour²⁸, we found that the recent evolution of increased parental care in the monogamous *P. polionotus* involved many regions spread across the genome. Most of these regions have sex-specific effects, suggesting that variation in male and female parental care has a different genetic basis, even if many of the behaviours appear similar between the sexes. Some brain sexual dimorphisms are thought to compensate for other biological differences between the sexes (like pregnancy and parturition only in females), ensuring that males and females behave similarly²⁹. Our results provide genetic evidence of this phenomenon: monogamous males and females evolve through different genetic routes to achieve similarly high levels of parental care.

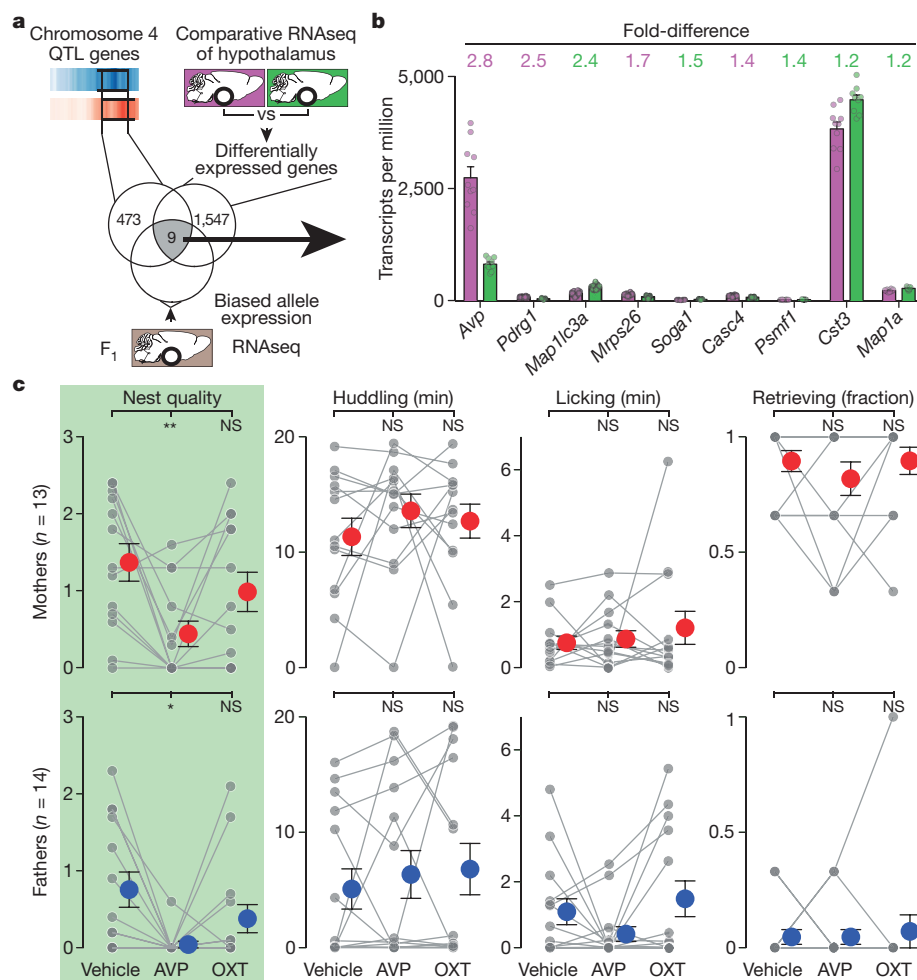


Figure 5 | Role for vasopressin in parental nest building. **a**, Twenty-three genes in the nest-building QTL on chromosome 4 are differentially expressed in the hypothalamus of the two species, 15 of which had interspecific variants required for allele-specific analysis in F₁ hybrids. **b**, Expression of the nine candidate genes from **a** in *P. maniculatus* (magenta) and *P. polionotus* (green) hypothalamus. The voom-transformed difference in expression is shown above; colour indicates

the species with higher expression. Circles represent each individual. No significant differences between sexes for any gene. **c**, Parental behaviours of *P. polionotus* after vehicle, 100 ng vasopressin (AVP), or 100 ng oxytocin (OXT) intracerebroventricular administration. Each individual (grey) is connected by lines. Red and blue circles with whiskers indicate mean \pm s.e.m. * $P < 0.05$; ** $P < 0.01$; NS, not significant by Friedman followed by Dunn's test compared with vehicle.

Ethological observations and theory^{30,31} as well as neurobiological experiments^{31,32} indicate that behaviours are often hierarchically organized such that an internal state (such as hunger) can motivate multiple specific behaviours related to that state (such as searching for and then consuming food). This organization is further manifested in the brain: some brain areas and neuron types contribute to the control of an entire suite of related behaviours, while other neurons control the execution of specific behaviours. For example, galanin neurons in the medial preoptic area of the hypothalamus are essential for multiple components of parental care³³, and more discrete neuronal types probably control the execution of each component. However, it is unknown how this hierarchical organization is manifested at the genetic level. Here we found genetic loci that affect parenting behaviour broadly, and others that are specific to a particular parenting behaviour sequence. Thus, the genetic architecture of parental behaviour mirrors its neuronal organization, and our results begin to provide novel molecular handles for multiple levels of this hierarchy, such as vasopressin and nest building.

It has long been argued that neurotransmitter and neuromodulator receptors are preferred targets of evolutionary change in behaviour because altering their expression pattern or levels can be more modular, hence less pleiotropic, than mutations in the respective ligands^{34,35}. Here we uncovered a case where differences in the levels of the

vasopressin peptide itself have probably contributed to interspecific variation in parental behaviour, arguing that, at least in some instances, genetic polymorphism affecting neuromodulators can contribute to behavioural evolution.

Our genetic dissection of parenting—from natural behaviour to candidate gene—opens exciting new avenues of research for the neurobiological and circuit-based understanding of a complex social behaviour. In particular, discovering molecular and neural mechanisms by which genes with sex-specific effects act to modulate behaviours common to both sexes, and how highly pleiotropic genes such as vasopressin may change only specific aspects of behaviour, represent important next steps in understanding how behaviours and the brain evolve.

Online Content Methods, along with any additional Extended Data display items and Source Data, are available in the online version of the paper; references unique to these sections appear only in the online paper.

Received 21 December 2016; accepted 16 March 2017.

Published online 19 April 2017.

- Lukas, D. & Clutton-Brock, T. H. The evolution of social monogamy in mammals. *Science* **341**, 526–530 (2013).
- Lim, M. M. *et al.* Enhanced partner preference in a promiscuous species by manipulating the expression of a single gene. *Nature* **429**, 754–757 (2004).

3. Okhovat, M., Berrio, A., Wallace, G., Ophir, A. G. & Phelps, S. M. Sexual fidelity trade-offs promote regulatory variation in the prairie vole brain. *Science* **350**, 1371–1374 (2015).
4. Wang, Z., Ferris, C. F. & De Vries, G. J. Role of septal vasopressin innervation in paternal behavior in prairie voles (*Microtus ochrogaster*). *Proc. Natl Acad. Sci. USA* **91**, 400–404 (1994).
5. Bosch, O. J. & Neumann, I. D. Both oxytocin and vasopressin are mediators of maternal care and aggression in rodents: from central release to sites of action. *Horm. Behav.* **61**, 293–303 (2012).
6. Dulac, C., O'Connell, L. A. & Wu, Z. Neural control of maternal and paternal behaviors. *Science* **345**, 765–770 (2014).
7. Scott, N., Prigge, M., Yizhar, O. & Kimchi, T. A sexually dimorphic hypothalamic circuit controls maternal care and oxytocin secretion. *Nature* **525**, 519–522 (2015).
8. Turner, L. M. *et al.* Monogamy evolves through multiple mechanisms: evidence from V1aR in deer mice. *Mol. Biol. Evol.* **27**, 1269–1278 (2010).
9. Birdsall, D. A. & Nash, D. Occurrence of successful multiple insemination of females in natural populations of deer mice (*Peromyscus maniculatus*). *Evolution* **27**, 106–110 (1973).
10. Dewsbury, D. A. Aggression, copulation, and differential reproduction of deer mice (*Peromyscus maniculatus*) in a semi-natural enclosure. *Behaviour* **91**, 1–23 (1984).
11. Dewsbury, D. A. & Lovecky, D. V. Copulatory behavior of old-field mice (*Peromyscus polionotus*) from different natural populations. *Behav. Genet.* **4**, 347–355 (1974).
12. Foltz, D. W. Genetic evidence for long-term monogamy in a small rodent, *Peromyscus polionotus*. *Am. Nat.* **117**, 665–675 (1981).
13. Dewsbury, D. A. An exercise in the prediction of monogamy in the field from laboratory data on 42 species of murid rodents. *Biologist* **63**, 138–162 (1981).
14. Peterson, B. K., Weber, J. N., Kay, E. H., Fisher, H. S. & Hoekstra, H. E. Double digest RADseq: an inexpensive method for de novo SNP discovery and genotyping in model and non-model species. *PLoS ONE* **7**, e37135 (2012).
15. Andolfatto, P. *et al.* Multiplexed shotgun genotyping for rapid and efficient genetic mapping. *Genome Res.* **21**, 610–617 (2011).
16. Royle, N. J., Smiseth, P. T. & Kölliker, M. *The Evolution of Parental Care* (Oxford Univ. Press, 2012).
17. Choi, Y., Sims, G. E., Murphy, S., Miller, J. R. & Chan, A. P. Predicting the functional effect of amino acid substitutions and indels. *PLoS ONE* **7**, e46688 (2012).
18. Lagoutte, E. *et al.* Oxidation of hydrogen sulfide remains a priority in mammalian cells and causes reverse electron transfer in colonocytes. *Biochim. Biophys. Acta Bioenerg.* **1797**, 1500–1511 (2010).
19. Seth, R. B., Sun, L., Ea, C.-K. & Chen, Z. J. Identification and characterization of MAVS, a mitochondrial antiviral signaling protein that activates NF- κ B and IRF 3. *Cell* **122**, 669–682 (2005).
20. Renella, R. *et al.* Codanin-1 mutations in congenital dyserythropoietic anemia type 1 affect HP1 α localization in erythroblasts. *Blood* **117**, 6928–6938 (2011).
21. Lindfors, P. H., Lindahl, M., Rossi, J., Saarma, M. & Airaksinen, M. S. Ablation of persephin receptor glial cell line-derived neurotrophic factor family receptor α 4 impairs thyroid calcitonin production in young mice. *Endocrinology* **147**, 2237–2244 (2006).
22. Numan, M. Medial preoptic area and maternal behavior in the female rat. *J. Comp. Physiol. Psychol.* **87**, 746–759 (1974).
23. Insel, T. R. & Harbaugh, C. R. Lesions of the hypothalamic paraventricular nucleus disrupt the initiation of maternal behavior. *Physiol. Behav.* **45**, 1033–1041 (1989).
24. Insel, T. R. The challenge of translation in social neuroscience: a review of oxytocin, vasopressin, and affiliative behavior. *Neuron* **65**, 768–779 (2010).
25. Kramer, K. M., Yamamoto, Y., Hoffman, G. E. & Cushing, B. S. Estrogen receptor α and vasopressin in the paraventricular nucleus of the hypothalamus in *Peromyscus*. *Brain Res.* **1032**, 154–161 (2005).
26. Neumann, I. D. & Landgraf, R. Balance of brain oxytocin and vasopressin: implications for anxiety, depression, and social behaviors. *Trends Neurosci.* **35**, 649–659 (2012).
27. Bult, A., van der Zee, E. A., Compaan, J. C. & Lynch, C. B. Differences in the number of arginine-vasopressin-immunoreactive neurons exist in the suprachiasmatic nuclei of house mice selected for differences in nest-building behavior. *Brain Res.* **578**, 335–338 (1992).
28. Bendesky, A. & Bargmann, C. I. Genetic contributions to behavioural diversity at the gene–environment interface. *Nat. Rev. Genet.* **12**, 809–820 (2011).
29. De Vries, G. J. Sex differences in adult and developing brains: compensation, compensation, compensation. *Endocrinology* **145**, 1063–1068 (2004).
30. Tinbergen, N. The hierarchical organization of nervous mechanisms underlying instinctive behaviour. *Symp. Soc. Exp. Biol.* **4**, 305–312 (1950).
31. Kennedy, A. *et al.* Internal states and behavioral decision-making: toward an integration of emotion and cognition. *Cold Spring Harb. Symp. Quant. Biol.* **79**, 199–210 (2014).
32. Devidze, N., Lee, A. W., Zhou, J. & Pfaff, D. W. CNS arousal mechanisms bearing on sex and other biologically regulated behaviors. *Physiol. Behav.* **88**, 283–293 (2006).
33. Wu, Z., Autry, A. E., Bergan, J. F., Watabe-Uchida, M. & Dulac, C. G. Galanin neurons in the medial preoptic area govern parental behaviour. *Nature* **509**, 325–330 (2014).
34. Insel, T. R., Gelhard, R. & Shapiro, L. E. The comparative distribution of forebrain receptors for neurohypophysal peptides in monogamous and polygamous mice. *Neuroscience* **43**, 623–630 (1991).
35. Donaldson, Z. R. & Young, L. J. Oxytocin, vasopressin, and the neurogenetics of sociality. *Science* **322**, 900–904 (2008).

Supplementary Information is available in the online version of the paper.

Acknowledgements E. Kingsley shared unpublished data. D. Stern, P. Andolfatto, and A. Kitzmiller helped implement MSG; V. Bajic helped with anchoring genomic scaffolds; M. Khadraoui with allele-specific expression analysis; K. Turner with ddRAD library construction. Computations were run on the Odyssey cluster supported by the Harvard FAS Research Computing Group. R. Hellmiss provided advice on figures. C. Bargmann and P. McGrath provided comments on the manuscript. This work was supported by a Helen Hay Whitney Foundation Postdoctoral Fellowship and a National Institutes of Health (NIH) K99 award HD084732 to A.B., Harvard Museum of Comparative Zoology Grants in Aid and Harvard Undergraduate Research Fellowships to Y.-M.K., a European Molecular Biology Organization (ALTF 379-2011), Human Frontier Science Program, and Belgian American Educational Foundation fellowships to J.-M.L., NIH training grant GM008313 (to M.X.H.), National Philanthropic Trust grant RFP-12-03 (to A.B. and H.E.H.), and a Harvard Mind Brain Behavior Award and Harvard Brain Science Initiative Grant to H.E.H. C.D. and H.E.H. are investigators of the Howard Hughes Medical Institute.

Author Contributions A.B. and H.E.H. conceived and designed the study. A.B. and Y.-M.K. collected and analysed behavioural data. A.B., Y.-M.K., and C.L.L. generated ddRAD-seq libraries. B.K.P. wrote code to map ddRAD-seq data. B.K.P. and A.B. wrote code to track animal behaviour from videos. A.B. and M.X.H. made a chromosome-level map of the *Peromyscus* genome. A.B. performed genetic mapping, pharmacology, and chemogenetics experiments. A.B. and J.-M.L. collected and analysed the RNA sequencing data. C.L.L. blind-scored behavioural assays. S.Y. made the *Avp-Cre* transgenic mice. A.B., Y.-M.K., J.-M.L., C.D., and H.E.H. analysed and interpreted results. A.B. and H.E.H. wrote the paper with input from all authors.

Author Information Reprints and permissions information is available at www.nature.com/reprints. The authors declare no competing financial interests. Readers are welcome to comment on the online version of the paper. Publisher's note: Springer Nature remains neutral with regard to jurisdictional claims in published maps and institutional affiliations. Correspondence and requests for materials should be addressed to H.E.H. (hoekstra@oeb.harvard.edu).

Reviewer Information *Nature* thanks S. Phelps and the other anonymous reviewer(s) for their contribution to the peer review of this work.

METHODS

Except where stated, no statistical methods were used to predetermine sample size, the experiments were not randomized, and the investigators were not blinded to allocation during experiments and outcome assessment.

Animal husbandry. We established colonies of *P. maniculatus bairdii* (strain BW) and *P. polionotus subgriseus* (strain PO) at Harvard University from animals originally obtained from the *Peromyscus* Stock Center at the University of South Carolina. We housed animals in barrier, specific-pathogen-free conditions with 16 h light: 8 h dark at 22 °C in individually ventilated cages (7.75" wide × 12" long × 6.5" high; Allentown, Allentown, New Jersey) with quarter-inch Bed-o-cob bedding (The Andersons, Maumee, Ohio). Breeding animals and their litters were fed irradiated PicoLab Mouse Diet 20 5058 (LabDiet, St. Louis, Missouri) *ad libitum* and had free access to water. We weaned animals at 23 days of age into cages with at most four other members of the same strain and sex. After weaning, we fed animals irradiated LabDiet Prolab Isopro RMH 3000 5P75 (LabDiet) *ad libitum* with free access to water and provided them with nesting material (Nestlet, Ancare, Bellmore, New York) and a polycarbonate translucent red hut. Animal experimentation protocols were approved by the Harvard University Faculty of Arts and Sciences Institutional Animal Care and Use Committee.

Parental behaviour assay. We tested animals for parental behaviour when their pups were 4, 5, and 6 days old. Parental behaviour was tested with the first litter unless otherwise noted. Testing was performed between zeitgeber times 6 and 15. We transferred animals to a testing room adjacent to the housing room. The female, pups, nest, red hut, and food hopper were transferred to a new cage and placed 30–300 cm from the male cage, undisturbed while the male was being tested.

To begin each assay (time 0), we gave ~0.625 g of compacted cotton nesting material (Ancare, Bellmore, New York) to the male within 1 min of being transferred to the test cage. At 30 min, we placed one of the animal's own pups inside the cage (in the centre of the cage if the male had built a nest in a corner or was sitting in a corner or in a corner if the animal had built a nest in the centre). We then scored the latency to approach the pup, to handle (move) the pup with the front paws, to lick the pup, to huddle over the pup (by covering at least 50% of the pup's body with the parent's body), and to retrieve the pup (pick up the pup with the mouth and displace it from its original position). We also scored the total time licking the pup and huddling over the pup until minute 50, when we scored nest quality according to the scale described below. At minutes 50 and 52 (20 and 22 min after adding the pup), we added another of the fathers' own pups to the cage (following the same placement guidelines as above and at least 5 cm from pups already in the cage) and scored the time to retrieve the pup. If there were fewer than three pups in the litter, we used one of the pups again (removing it at minutes 50 and 52), waiting 10–15 s before adding it back to the cage to measure retrieval. We tested female mice in a similar fashion, after the male, in the new cage where she had been placed at the beginning of the assay.

The experimenter scored each assay ~200 cm from the cage by observing the cage and a monitor with a video feed from the side of the cage opposite to the experimenter. This double view facilitated scoring of all behaviours, particularly huddling and licking. In Figs 1 and 2, we used the median of the three tests for each behavioural parameter. To increase genetic mapping resolution by avoiding ties in the F₂ mice, however, we used the mean of the three tests.

Nest quality score. We used the following scoring system to quantify nest-building behaviour: 0, nesting material is not shredded; 1, all of the nesting material is shredded but is scattered; 2, nesting material is shredded and gathered in a flat platform; 3, nesting material is shredded and has enough height to cover the entire animal; 4, nest covers the entire animal including a complete roof. Nests that were between two of the above categories received an intermediate score in increments of 0.1.

Home cage long-term behavioural observations. We set up breeding cages as described above in the Animal husbandry section. Two days before their first litter, we attached three cameras (Microsoft LifeCam HD-5000, with the infrared cut filter removed, adapted with a 180° 0.25 × fisheye lens, and a Neewer 720 nm long-pass filter over the fisheye lens) to the cage. Two cameras were inside the cage, above the food hopper, and one camera was outside the cage, on one side, focused on the nest. We illuminated the cage with a strip of infrared light-emitting diodes attached to the outside of the cage, near the top. To provide a better view of the parents and pups, we removed part of the nest, leaving enough nesting material for a nest with walls but not enough for a roof. The cameras were connected to a computer that recorded continuously with a custom Python script from before birth to 3 days after birth.

We scored the following behaviours on the video recordings, sampling 5 min from every hour at 1 h intervals: amount of time in and outside the nest, time licking pups, time huddling over the pups, time building nest, time retrieving pups, time grooming their mate.

Cross-fostering experiments. Within 24 h of birth, we exchanged pups from one species (*P. polionotus* or *P. maniculatus*) with pups of the other species that were also born within 24 h. In no case was there any obvious rejection of the pups. We weaned cross-fostered pups at 23 days of age with pups of their biological species in cages of five animals of the same sex, in the same way as non-cross-fostered animals. At 60–90 days old, we paired cross-fostered animals with an animal of their own biological species (cross-fostered or not) and tested parental behaviours as described above. Numbers of litters from which cross-fostered animals were derived: *P. polionotus* mothers, 8; fathers, 9; *P. maniculatus* mothers, 9; fathers, 7.

Cross design. To generate a genetically heterogeneous F₂ hybrid population, we first mated four *P. maniculatus* females to four *P. polionotus* males. We were limited to only a single cross direction because of excessive fetal growth and the resultant death of mothers when *P. polionotus* females are mated with *P. maniculatus* males³⁶. Next, 16 F₁-sib pairs were intercrossed to generate 769 F₂ hybrids. These F₂ individuals have autosomes that are a recombinant mix of the two species as well as the *P. maniculatus* mitochondria, and males carry the *P. polionotus* Y chromosome. **ddRAD-seq.** We performed ddRAD-seq as described in ref. 14, with some modifications. In brief, we extracted DNA from a liver sample using an AutoGenprep 965 (Autogen). Next, we digested DNA with MluCI and NlaIII enzymes (New England Biolabs), ligated fragments to biotinylated barcoded adapters, and combined them in pools of ≤48 samples. Using a Pippin Prep (Sage Science), we selected fragments of 216–276 base pairs (bp) and purified biotinylated fragments with streptavidin beads, then PCR amplified each pool using a different Illumina multiplex read index for ten cycles using Phusion (New England Biosciences). We evaluated the quality of the final libraries in a 2200 TapeStation (Agilent Technologies) and quantified them fluorimetrically with a Qubit 2.0 (Thermo Fisher Scientific).

We sequenced 384 individuals per lane of an Illumina HiSeq 2500 with HiSeq version 4 chemistry in high output mode and paired-ends (2 × 125 bp) to a median depth of 7.8 × 10⁵ reads per individual. We then processed Illumina fastq files into separate files on the basis of Illumina multiplex read indices. We merged and trimmed overlapping paired-ends to remove adaptor sequence readthrough and then further de-multiplexed on the basis of the custom barcode.

Overlapping reads were mapped to the *P. maniculatus bairdii* (strain BW) genome reference (Pman_1.0, GenBank assembly accession: GCA_000500345.1) using BWA 0.7.5a (ref. 37) and then re-mapped using Stampy 1.0.18 (ref. 38). Using GATK 2.7-2, we re-aligned reads and called genotypes using UnifiedGenotyper³⁹.

Chromosome-level map of *P. maniculatus* genome. The *P. maniculatus bairdii* (BW) draft reference genome (Pman_1.0, GenBank assembly accession: GCA_000500345.1) has a total sequence length of 2,630,541,020 bp and is assembled into 30,921 scaffolds with a N50 of 3,760,915 bp. To anchor scaffolds into chromosomes, we used genetic linkage data, which reflect the ordering and relative orientation of scaffolds in each linkage group. The procedure involved the following steps.

1. To minimize conflicts in genetic linkage arising from translocations, inversions, and other structural variants that could arise in an interspecific cross, we used genetic information from an intraspecific cross between *P. maniculatus bairdii* (BW) and *P. maniculatus nubiterrae* (NUB) from Pennsylvania (E. Kingsley, unpublished observations). We genotyped 403 F₂ individuals with ddRAD-seq, using EcoRI–NlaIII fragments of 216–276 bp. After quality filtering (quality by depth (QD) > 5, genotype quality (GQ) > 20, removing markers with identical genotypes in all F₂ mice, and markers with genotypes in fewer than 220 F₂ mice), we obtained 1,779 high-confidence markers.

2. A genetic map was constructed from these 1,779 markers using R/qtl and marker ordering was optimized following guidelines from <http://www.rqtl.org/tutorials/geneticmaps.pdf>. This produced a map with 23 autosomal linkage groups as expected on the basis of the number of *P. maniculatus* chromosomes^{40,41}. The X chromosome markers were identified via model-based clustering that used the heterozygote frequencies of markers in males and in females, using the Mclust function in the mclust package in R⁴². We assigned 130 markers to the X chromosome and determined their order as we did for the autosomes.

3. We ordered the 557 scaffolds represented by these 1,779 markers on the basis of the relative position of the markers and oriented them whenever there was more than one marker per scaffold. Spacing between scaffolds was based on the median genetic to physical distance correspondence of 1.4 centimorgans per megabase calculated with the scaffolds with more than one marker.

4. This chromosome-level map was used for MSG genotyping of the *P. maniculatus* × *P. polionotus* F₂ hybrids. The recombination fraction plots were examined in detail using plotRF (R/qtl) and iplotRF (R/qtlcharts⁴³), and scaffolds were moved to a place with higher linkage and reoriented, whenever possible. This generated a new map that was used for a new MSG run and further

improvement of the scaffold coordinates. This cycle was repeated 13 times, when no further improvement was seen. At this point, the 557 scaffolds encompassed 1,872,038,949 bp, or 71% of the total sequence in the Pman_1.0 assembly.

5. To add additional scaffolds (and thus include a larger fraction of the genome) to our chromosome-level map, we genotyped 614 *P. maniculatus* × *P. polionotus* F₂ hybrids using high-confidence GATK genotypes (filtered depth of coverage at the sample level, DP > 7) directly (as opposed to genotype probabilities from MSG), from ddRAD libraries sequenced at higher coverage. We then mapped these markers into the existing genetic map using Haley–Knott regression. This procedure allowed us to add 1,166 scaffolds to the map.

6. Scaffold coordinates (chromosomal location and orientation) were optimized as described in step 4, eight times, when no further improvement was seen.

7. We assigned chromosome names to the linkage groups in our map on the basis of the localization of known genes in *Peromyscus* chromosomes in our linkage groups⁴⁴. Chromosomes 16 and 21 from ref. 44 are represented by a single linkage group in our map, and there was no obvious position to split this linkage group, as there was strong linkage among markers throughout. On the basis of new data from fluorescence hybridization experiments (M. Felder and R. O'Neill, personal communication), we find that chromosome 8a (from ref. 44) actually corresponds to chromosome 16, 8b (from ref. 44) is chromosome 8, and in agreement with our linkage results, chromosomes 16 and 21 (from ref. 44) should both be included in chromosome 21. The chromosome names reported here reflect this updated nomenclature.

Our map includes 1,723 scaffolds, which encompass 2,444,934,125 bp (93% of the total sequence in Pman_1.0), in 23 autosomes and the X chromosome (Supplementary Data File 2). Genetic linkage data suggests that 63 scaffolds are erroneous chimaeras, since different parts of those scaffolds map to different chromosomes or different parts of a single chromosome.

MSG. To identify variants fixed between the *P. maniculatus* and *P. polionotus* founders of our intercross, we performed ddRAD-seq in eight founders of the cross (four per species). We used Picard (<http://broadinstitute.github.io/picard/>) to merge the reads of the four animals of each species into one pseudo-individual of each species and then used GATK 2.7-2 UnifiedGenotyper to genotype the two pseudo-individuals. Variants called at GQ > 15 that were opposite homozygotes in the two pseudo-individuals amounted to a preliminary set of 961,137 fixed variants. To eliminate variants that were not fixed, we genotyped 614 of the F₂ mice in additional HiSeq lanes (as described above) to a median depth of 1×10^6 reads per individual. Only one-quarter of the F₂ mice were expected to be homozygous at a given variant, so we removed the 124,629 variants that were homozygous in all F₂ mice genotyped at that position with a DP ≥ 7. This left us with a set of 836,508 fixed variants.

Next, we performed MSG as described in ref. 15, with some modifications. From Samtools⁴⁵ mpileups of the GATK RealignedReads BAMs, we extracted the fixed variants and kept only those that were separated by at least 1 kilobase (kb), thus ensuring they originated from independent reads. We formatted these filtered mpileups to be compatible with the hidden Markov model (fit-hmm.R) step of MSG and started the MSG pipeline at that step. Before running fit-hmm, the variants in each scaffold were combined into chromosomes on the basis of the coordinates from our chromosome-level assembly (described above). We used the following settings in fit-hmm: *deltapar1* 0.015; *deltapar2* 0.015; *recRate* 25; *rfac* 1; *priors* 0.25,0.5,0.25; *priors* for X chromosome in females 0.5,0.5,0.0; *theta* 1; *one_site_per_contig* 1. We combined fit-hmm data of all F₂ mice using *combine.py* (<https://github.com/janeliaSciComp/msg/>), which yielded 406,611 variants. Many of these variants contained redundant information, because there was no recombination between them. Therefore, we filtered variants to include only neighbouring markers with a genotype conditional probability that differed by at least 0.1, using *pull_thin* (https://github.com/dstern/pull_thin)⁴⁶ with the following settings: *diffac* = 0.1; *chroms* = all; *cross* = f2; *autosome_prior* = 0.25; *X_prior* = 0.25. This procedure yielded 56,068 variants that were used for QTL analysis.

QTL analysis. We calculated that 350 F₂ hybrids per sex would provide 90% power at a 5% false positive rate to detect QTLs that individually explained ≥4% of the variance in behaviours among the F₂ mice (in each sex)⁴⁷. For QTL analysis, we used R/qtl⁴⁸. Ancestry probabilities of the 769 F₂ mice were imported into R/qtl as genotype probabilities using *read.cross.msg.1.5.R* (https://github.com/dstern/read_cross_msg/)⁴⁶. We performed non-parametric interval mapping separately on males and females. We determined significance thresholds by 1,000 permutations of the data using *scanone*. We also performed additional scans to search for QTLs with different effects in the two sexes using Haley–Knott regression on nqrnk normalized traits, using sex as an interactive and an additive covariate and subtracting the lod scores from a scan with sex as an additive covariate alone. For permutations to determine significance thresholds, we used the same random seed for both of these scans. We calculated the variance explained by the QTL of

nqrnk normalized values in F₂ mice using $1 - 10^{-2lod/n}$ as implemented in *fitqtl* from R/qtl.

Comparative transcriptomics. To estimate mRNA abundance in whole hypothalamus of *P. maniculatus* and *P. polionotus*, we conducted an RNA sequencing (RNA-seq) experiment. Specifically, immediately after a parental behaviour assay on the sixth day after the birth of their litter, we euthanized five male and five female parents by CO₂ inhalation for 2 min and collected hypothalami according to ref. 49. We immersed the tissue in ice-cold TRIzol reagent (Thermo Fisher, Waltham, Massachusetts) and disrupted the tissues with a motorized pestle before storage at −80 °C until processing. Hypothalamus samples from males and females from both species were processed together from RNA extraction to sequencing to alleviate batch effects. Total RNA was extracted using Direct-zol-96 RNA (Zymo Research, Irvine, California) and used as input to isolate messenger RNA with a NEB magnetic mRNA isolation kit (New England Biolabs, Ipswich, Massachusetts). We constructed complementary DNA (cDNA) libraries using the NEBNext Ultra Directional RNA Library Prep Kit for Illumina (NEB, Ipswich, Massachusetts). Multiplexed libraries were sequenced on an Illumina HiSeq 2500 (Illumina, San Diego, California) with HiSeq version 4 chemistry in high output mode and paired-ends (2 × 125 bp). Libraries from males and females from both species were sequenced in the same lanes to alleviate batch effects. The average depth per sample was 46.1 million reads. We removed low-quality and adaptor bases from raw reads using TrimGalore v0.4.0 (http://www.bioinformatics.babraham.ac.uk/projects/trim_galore/) and mapped the cleaned reads to the genome using the STAR RNA-Seq aligner version 2.4.2a in two-pass mode⁵⁰. We obtained the *P. maniculatus* genome sequence and annotation from the *Peromyscus* Genome Project (Pman_1.0, GenBank accession number GCA_000500345.1). We created a *P. polionotus* genome and annotation by incorporating single nucleotide polymorphism (SNPs) and indels into the *P. maniculatus* Pman_1.0 reference using the AlleleSeq package⁵¹ and the UCSC liftover tool. Briefly, *P. polionotus* genomic DNA reads (GenBank BioProject accession number PRJNA53593) were aligned to the Pman_1.0 reference using Stampy³⁸ version 1.0.21 with a substitution rate = 0.04. The resulting alignment files were pre-processed according to the GATK Best Practices. We used Haplotype Caller to perform variant calling as implemented in GATK 3.3-0 and filtered out variants with non-reference allele frequency < 0.50.

We estimated expression using STAR alignments in transcriptomic coordinates and the RSEM package⁵², and calculated differential expression using the limma package following voom transformation of the estimated counts^{53,54}. Raw read counts for genes with at least one count per million in at least three samples (15,729 genes) were used as inputs to the limma/voom pipeline, and scale normalization of the RNA-seq read counts was performed using the TMM normalization method⁵⁵. The Benjamini and Hochberg method⁵⁶ was used for adjusting for multiple testing, and we report values of expression at an FDR of 5% for the species factor in a linear model that included species, sex, and species × sex as factors.

Allele-specific expression analysis. We crossed two *P. maniculatus* females to two *P. polionotus* males to produce F₁ hybrids. Then, we dissected the hypothalamus of six female and six male adult F₁ offspring. We used the same procedure described above to sequence RNA libraries. Then we aligned the quality and adaptor trimmed reads to a hybrid diploid *P. maniculatus*/*P. polionotus* genome using STAR version 2.4.2a (ref. 50). For each gene, we selected variants common to all isoforms and kept only the variants that were homozygous for opposite alleles in the two species. Of the 23 genes that were differentially expressed between *P. maniculatus* and *P. polionotus* and present in the chromosome 4 nest-building QTL, 15 had variants that allowed us to distinguish the species of origin of the transcripts in the F₁ hybrids. We counted the number of reads containing the *P. maniculatus* allele or the *P. polionotus* allele in the F₁ hybrids. Using one to three variants per gene represented by different reads, we fitted a linear model for each gene in the R package $\text{lm}(\ln(\text{maniculatus mapping reads}) - \ln(\text{polionotus mapping reads})) \sim \text{sex}$, where ‘~’ represents linear predictor, and identified genes with significant differences in allele-specific expression at an FDR of 5%.

To perform allele-specific expression analysis of *Avp* by droplet-digital PCR (ddPCR), we extracted RNA from whole brain or from specific brain regions. We extracted RNA from whole brain RNA using TRIzol and chloroform, cleaned the RNA using Qiagen RNeasy columns, and made cDNA with Quanta qScript cDNA Supermix followed by DNaseI digestion. To microdissect individual vasopressin-producing nuclei, we froze freshly dissected brains in Tissue-Tek O.C.T. Compound over dry ice, then mounted brains in cryostat, sectioned coronally until we reached the most posterior part of the anterior commissure, and finally made 1 mm diameter, ~1.5 mm thick punches with the aid of a stereo microscope (Extended Data Fig. 8a). We quickly froze these punches in an RNAlater-Micro Total RNA Isolation Kit (Ambion) lysis solution on dry ice, and extracted

RNA following the manufacturer's protocol. Finally, we made cDNA followed by DNaseI digestion using Superscript VILO (Invitrogen).

We used a BioRad QX200 Droplet Generator to create droplets, BioRad S1000 for PCR, a QX200 Reader to read droplets, and BioRad ddPCR Supermix for probes (No dUTP), all according to the manufacturer's instructions.

We used a TaqMan SNP Genotyping assay (Thermo Fisher) targeting the *Avp* SNP (*P. maniculatus* = C, *P. polionotus* = T) at position NW_006501268.1:1,146,329: primer 1, CCTAATGCTCGCCAGAATGCT; primer 2, CAGCAGGCTCAGGAAGCAA; reporter 1, AACGCCACGCTGTCT; reporter 2, AACGCCACACTGTCT.

Protein-coding variant analysis. For variant calling using the hypothalamus RNA-seq data, we mapped the cleaned reads from *P. maniculatus* and *P. polionotus* to the Pman_1.0 reference genome using STAR RNA-Seq aligner version 2.4.2a in two-pass mode and applying a mapping quality (MAPQ) of 60 for uniquely mapped reads. The resulting alignment files were pre-processed according to the GATK Best Practices recommendations for calling variants on RNA-seq data. Briefly, duplicate reads were marked using Picard (version 1.115) and reads spanning introns were split into exon segments using the SplitNCigarReads function of GATK. Next, we used HaplotypeCaller to perform variant calling as implemented in GATK 3.3-0 on each sample separately using the GVCF mode. Joint genotyping was subsequently performed using all gvcf files simultaneously, allowing a maximum of 12 alternate alleles. We used SnpEff version 4.3 (ref. 57) to annotate and predict the effects of variants on genes.

From the SnpEff-annotated vcf, we determined the genes with fixed differences between the species. A total of 21,316 protein-coding genes out of 22,720 in the annotation had variants that passed our quality filters (GATK's Best Practices: QD >2; FS <30; DP >4), indicating we could determine variation in 94% of genes in the genome using hypothalamus RNA-seq. To be considered a fixed difference, variants had to be called in at least three individuals of the ten per species, be homozygous in all called individuals, and have different alleles in the two species; these variants were all confirmed with DNA sequences of one independent *P. maniculatus* and one *P. polionotus* animal. To identify variants that affected protein sequences, we used SnpEff to select variants with MODERATE or HIGH putative impact. To evaluate the potential impact of fixed variants on protein function, we used the standalone version of the PROVEAN algorithm (version 1.1.5)¹⁷ and the NCBI nr database (downloaded April 2015).

Elevated plus maze assay. We designed an elevated plus maze that included four arms (31 cm length × 5 cm width), two closed arms with walls 15 cm high, and the maze floor raised 55 cm above the ground. We first used 50- to 60-day-old *P. maniculatus* and *P. polionotus* mice that were housed with same-sex animals. Testing was performed between zeitgeber times 8 and 15 with the lights on. We transferred animals in their home cage into the behaviour testing room, where they acclimated for 30 min before testing. To start a trial, we placed an animal inside a 34" × 1" × 3" red box, which we gently lowered into a closed arm of the maze. We left the animal inside the box for 2 min before releasing it in the centre of the maze by opening the door and removing the box without handling the animal. This approach—as opposed to transferring an animal directly from its home cage to the maze—reduced the number of times *Peromyscus* mice jumped off the maze at the start of a trial. We video-recorded the next 5 min and used custom code to track the position of the animal. The same assay was then used to measure anxiety-related behaviour in the 769 F₂ hybrid mice.

Intracerebroventricular drug delivery. Two to five days before the birth of a litter of *P. polionotus* pairs, we implanted guide cannulas in the right lateral cerebral ventricle (coordinates from bregma: mediolateral, 1 mm; dorsoventral, 1.8 mm; anteroposterior, +0.1) under isoflurane anaesthesia and using topical incisional bupivacaine and subcutaneous buprenorphine as analgesics. We used C315GAS-5 26-gauge cannulas (Plastics One) cut 1.8 mm below pedestal and covered the cannula with C315DCS-5 dummy cannulas that fit the guide cannulas without projecting. Six pairs had to be separated after surgery because they chewed on the cannulas of their mate. In those cases, we used an acrylic divider with multiple slits to separate the animals in their home cage but allowing for nose protrusion to the other side of the cage.

A day after a litter was born, we administered 2 μl Ringer's solution (NaCl 7.2 g l⁻¹, CaCl₂ 0.17 g l⁻¹, KCl 0.37 g l⁻¹, pH 7.35) via a C315IAS-5 33-gauge internal cannula protruding 0.5 mm below guide cannula, at a rate of 0.75 μl min⁻¹ using a MyNeuroLab syringe pump under light (1.5% isoflurane) anaesthesia. Immediately after intracerebroventricular delivery, we performed a standard parental behaviour assay as described above, except the acclimation period before a pup was introduced was reduced to 15 min. We selected this interval between drug delivery and behavioural test to match the pharmacokinetics—the half-life of vasopressin in cerebrospinal fluid is 24 min (ref. 58) and the physiological effects of intracerebroventricular vasopressin start within 10 min of administration for the dose we used and recover by 1 h (ref. 59). A day later, animals received an intracerebroventricular injection of 100 ng vasopressin

(Tocris) in Ringer's solution. The next day, animals received an intracerebroventricular injection of 100 ng oxytocin (Tocris) in Ringer's solution. All compounds were injected in a 2 μl volume as described above for the vehicle control (Ringer's solution) and doses were within the range of those used previously in rodents^{59–63}. We checked the correct placement of the cannulas by delivering Chicago Sky blue solution after the last test and visually confirming the presence of dye in the brain ventricles.

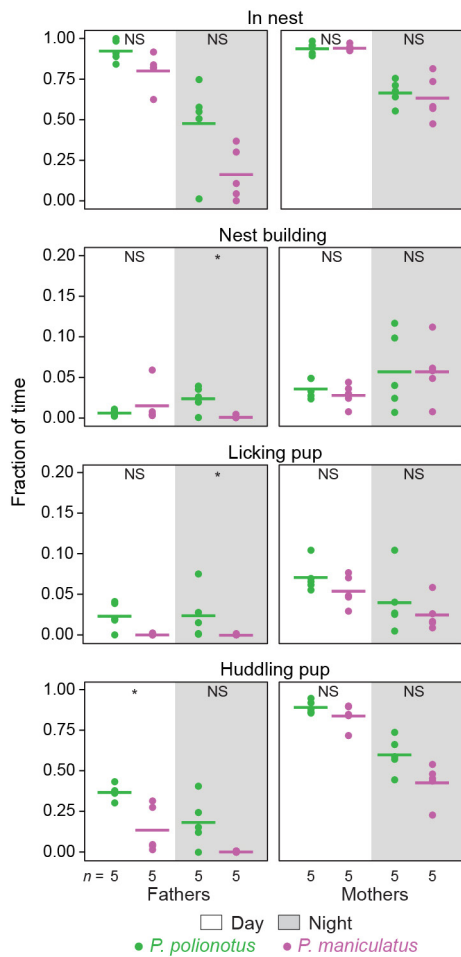
Generation of transgenic mice. To generate recombinant bacterial artificial chromosome (BAC) constructs, we used the RP23-152M19 and RP24-63F7 BAC clones, in which the *Avp* coding sequences are flanked by ~90 kb and ~60 kb genomic sequences on each side. An IRES-Cre cassette was inserted immediately after the stop codon of the *Avp* sequence in the BAC clones by homologous recombination. We mixed equal amounts of modified BAC constructs derived from RP23-152M19 and RP24-63F7 and then microinjected the mix into pronuclei of B6/CBA F₁ oocytes to generate transgenic founders. We backcrossed founders to C57BL6/J mice for five generations before testing. The transgene was inserted in the X chromosome; we used homozygous females and hemizygous males for all experiments. We verified Cre expression in vasopressin cells by immunofluorescence staining in two animals of each sex (Cre antibody: EMD Millipore MAB3120; vasopressin antibody: Immunostar 20069), as shown in Extended Data Fig. 10a. In males, 94.4% of 213 vasopressin⁺ cells were Cre⁺ in the PVN and 97.7% of 221 cells in the SON; 99.5% of 202 Cre⁺ cells were vasopressin⁺ in the PVN and 97.7% of 221 cells in the SON. In females, 96.9% of 213 vasopressin⁺ cells were Cre⁺ in the PVN and 97.7% of 221 cells in the SON; 99.5% of 202 Cre⁺ cells were vasopressin⁺ in the PVN and 97.7% of 221 cells in the SON.

Chemogenetics. We obtained recombinant adeno-associated viruses from the Penn Vector Core (University of Pennsylvania). We injected 200 nl of either rAAV-hSyn-DIO-hM4D(Gi)-mCherry (Gi-DREADD) or rAAV-hSyn-DIO-hM3D(Gq) (Gq-DREADD) stereotactically into the PVN of 2- to 4-month-old *Avp-Cre* transgenic mice, bilaterally (from bregma, -0.9 mm anteroposterior, 4.75 mm dorsoventral, ±0.25 mm mediolateral). Three to 4 weeks later, we injected mice intraperitoneally with 0.9% NaCl (10 μl per g body weight) and placed them in a clean mouse cage with corncob bedding, 2.5 g of cotton nestlet, and ~3 ml hydrogel. We covered the cage with a clear Plexiglass lid and recorded the animal for 1 h. Two to 4 days later, we tested mice again, this time after an intraperitoneal injection of clozapine-N-oxide (Sigma) (10 mg per kg in 0.9% NaCl, 10 μl per g body weight). Two to 4 days later, we tested mice after an intraperitoneal injection of 0.9% NaCl, as in the first day. An experimenter blind to the sex of the animal, type of rAAV used, and the intraperitoneal injection received, scored the time spent shredding, rearranging, and retrieving nesting material on randomized videos. We verified the delivery of the virus by histology, and present data for mice with DREADD-mCherry expression bilaterally in the PVN and not in the supraoptic nucleus, suprachiasmatic nucleus, bed nucleus of the stria terminalis, or medial amygdala.

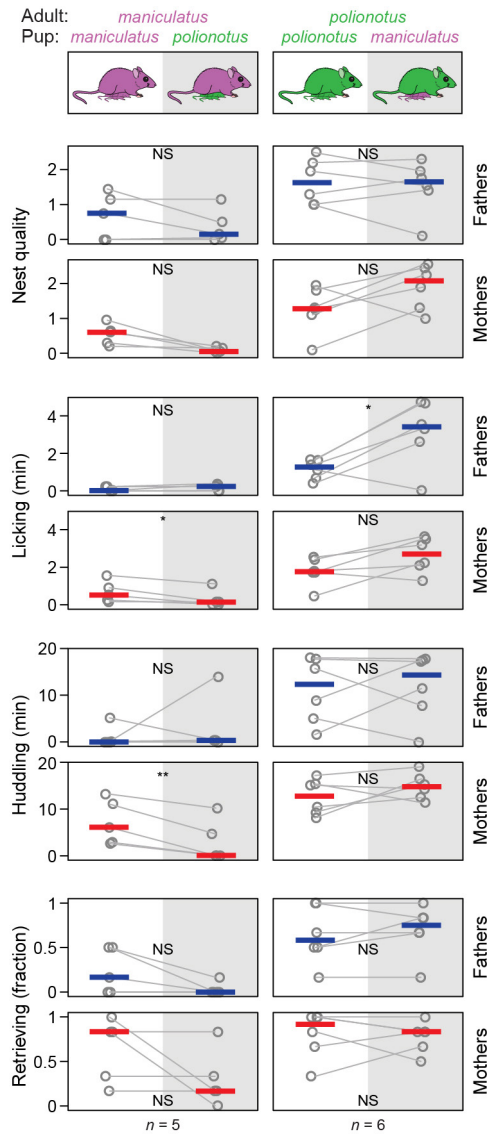
Data availability. RNA-seq data have been deposited in the NCBI Sequence Read Archive (BioProject PRJNA376410). Other datasets reported in this study are provided as Source Data and Supplementary Data.

- Dawson, W. D. Fertility and size inheritance in a *Peromyscus* species cross. *Evolution* **19**, 44–55 (1965).
- Li, H. & Durbin, R. Fast and accurate short read alignment with Burrows-Wheeler transform. *Bioinformatics* **25**, 1754–1760 (2009).
- Lunter, G. & Goodson, M. Stampy: a statistical algorithm for sensitive and fast mapping of Illumina sequence reads. *Genome Res.* **21**, 936–939 (2011).
- Van der Auwera, G. A. et al. From FastQ data to high confidence variant calls: the Genome Analysis Toolkit best practices pipeline. *Curr. Protoc. Bioinformatics* **11**, 11.10.1–11.10.33 (2013).
- Painter, T. S. A comparative study of the chromosomes of mammals. *Am. Nat.* **59**, 385–409 (1925).
- Greenbaum, I. F. et al. Cytogenetic nomenclature of deer mice, *Peromyscus* (Rodentia): revision and review of the standardized karyotype. Report of the Committee for the Standardization of Chromosomes of *Peromyscus*. *Cytogenet. Cell Genet.* **66**, 181–195 (1994).
- Fraley, C. & Raftery, A. *mclust version 4 for R: normal mixture modeling for model-based clustering, classification, and density estimation* (Department of Statistics, University of Washington, 2012).
- Broman, K. W. R/qtlcharts: interactive graphics for quantitative trait locus mapping. *Genetics* **199**, 359–361 (2015).
- Kenney-Hunt, J. et al. A genetic map of *Peromyscus* with chromosomal assignment of linkage groups (a *Peromyscus* genetic map). *Mamm. Genome* **25**, 160–179 (2014).
- Li, H. et al. The Sequence Alignment/Map format and SAMtools. *Bioinformatics* **25**, 2078–2079 (2009).
- Cande, J., Andolfatto, P., Prud'homme, B., Stern, D. L. & Gompel, N. Evolution of multiple additive loci caused divergence between *Drosophila yakuba* and *D. santomea* in wing rowing during male courtship. *PLoS ONE* **7**, e43888 (2012).

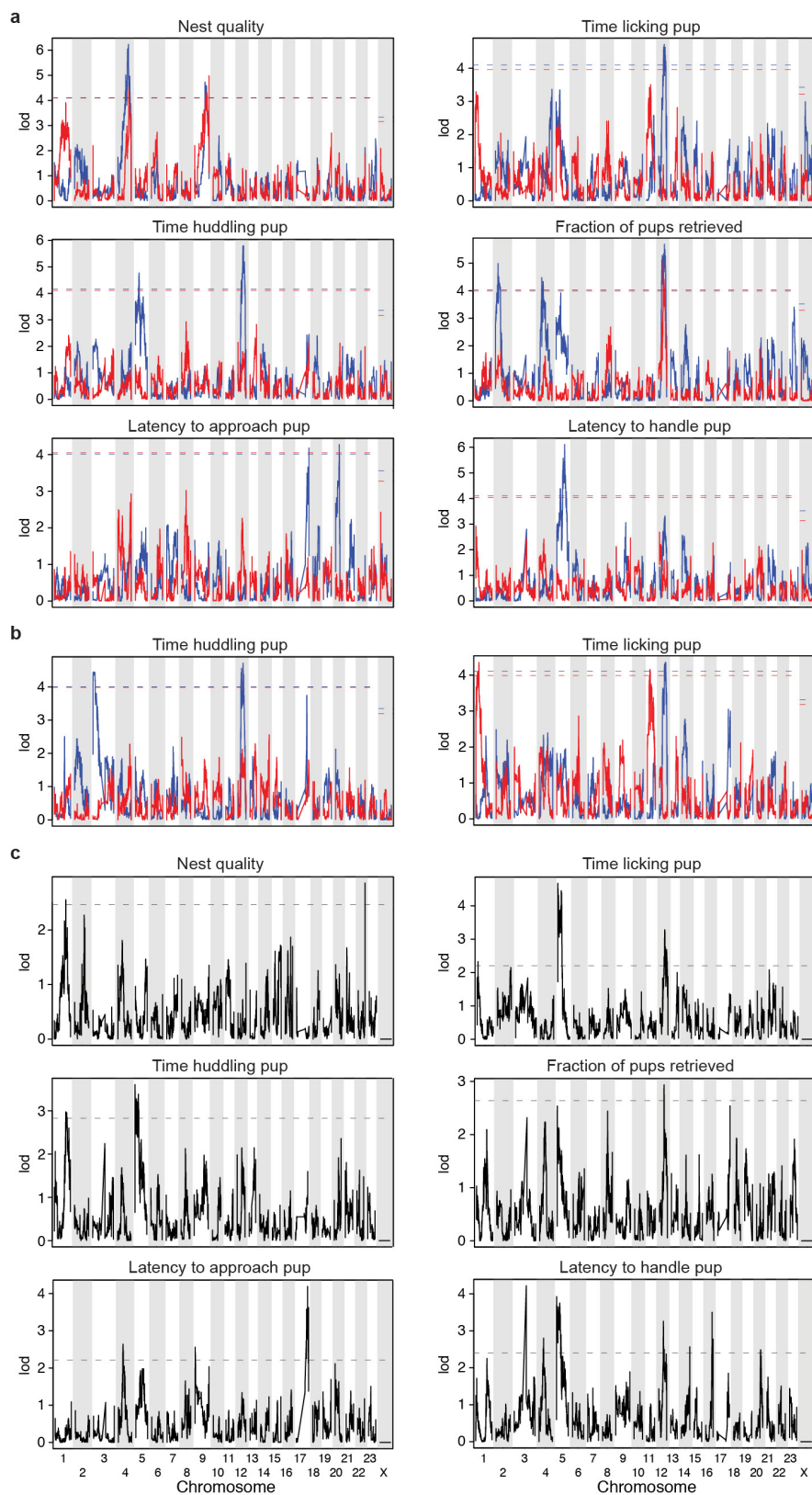
47. Lynch, M & Walsh, B. *Genetics and Analysis of Quantitative Traits* 469–476 (Sinauer, 1998).
48. Broman, K. W., Wu, H., Sen, S. & Churchill, G. A. R/qtl: QTL mapping in experimental crosses. *Bioinformatics* **19**, 889–890 (2003).
49. Zapala, M. A. *et al.* Adult mouse brain gene expression patterns bear an embryologic imprint. *Proc. Natl Acad. Sci. USA* **102**, 10357–10362 (2005).
50. Dobin, A. *et al.* STAR: ultrafast universal RNA-seq aligner. *Bioinformatics* **29**, 15–21 (2013).
51. Rozowsky, J. *et al.* AlleleSeq: analysis of allele-specific expression and binding in a network framework. *Mol. Syst. Biol.* **7**, 522 (2011).
52. Li, B. & Dewey, C. N. RSEM: accurate transcript quantification from RNA-Seq data with or without a reference genome. *BMC Bioinformatics* **12**, 323 (2011).
53. Ritchie, M. E. *et al.* limma powers differential expression analyses for RNA-sequencing and microarray studies. *Nucleic Acids Res.* **43**, e47 (2015).
54. Law, C. W., Chen, Y., Shi, W. & Smyth, G. K. voom: precision weights unlock linear model analysis tools for RNA-seq read counts. *Genome Biol.* **15**, R29 (2014).
55. Robinson, M. D. & Oshlack, A. A scaling normalization method for differential expression analysis of RNA-seq data. *Genome Biol.* **11**, R25 (2010).
56. Benjamini, Y. & Hochberg, Y. Controlling the false discovery rate: a practical and powerful approach to multiple testing. *J. R. Stat. Soc. B* **57**, 289–300 (1995).
57. Cingolani, P. *et al.* A program for annotating and predicting the effects of single nucleotide polymorphisms, SnpEff. *Fly* **6**, 80–92 (2012).
58. Clark, R. G., Jones, P. M. & Robinson, I. C. A. F. Clearance of vasopressin from cerebrospinal fluid to blood in chronically cannulated Brattleboro rats. *Neuroendocrinology* **37**, 242–247 (1983).
59. Diamant, M. & De Wied, D. Differential effects of centrally injected AVP on heart rate, core temperature, and behavior in rats. *Am. J. Physiol.* **264**, R51–R61 (1993).
60. Pedersen, C. A., Ascher, J. A., Monroe, Y. L. & Prange, A. J., Jr. Oxytocin induces maternal behavior in virgin female rats. *Science* **216**, 648–650 (1982).
61. Fahrbach, S. E., Morrell, J. I. & Pfaff, D. W. Oxytocin induction of short-latency maternal behavior in nulliparous, estrogen-primed female rats. *Horm. Behav.* **18**, 267–286 (1984).
62. Winslow, J. T., Hastings, N., Carter, C. S., Harbaugh, C. R. & Insel, T. R. A role for central vasopressin in pair bonding in monogamous prairie voles. *Nature* **365**, 545–548 (1993).
63. Kessler, M. S., Bosch, O. J., Bunck, M., Landgraf, R. & Neumann, I. D. Maternal care differs in mice bred for high vs. low trait anxiety: impact of brain vasopressin and cross-fostering. *Soc. Neurosci.* **6**, 156–168 (2011).
64. Bosch, O. J. & Neumann, I. D. Brain vasopressin is an important regulator of maternal behavior independent of dams' trait anxiety. *Proc. Natl Acad. Sci. USA* **105**, 17139–17144 (2008).
65. Kuroda, K. O., Tachikawa, K., Yoshida, S., Tsuneoka, Y. & Numan, M. Neuromolecular basis of parental behavior in laboratory mice and rats: with special emphasis on technical issues of using mouse genetics. *Prog. Neuropsychopharmacol. Biol. Psychiatry* **35**, 1205–1231 (2011).
66. Xu, X. *et al.* Modular genetic control of sexually dimorphic behaviors. *Cell* **148**, 596–607 (2012).



Extended Data Figure 1 | Parental behaviours in undisturbed home cages for 3 days after the birth of a litter. The fraction of time an animal was engaged in each behaviour averaged across 5-min samples for each hour, for the 16 h of light and 8 h of dark parts of the day separately. Horizontal lines denote the mean. * $P < 0.05$; NS, not significant by Mann-Whitney U -test.



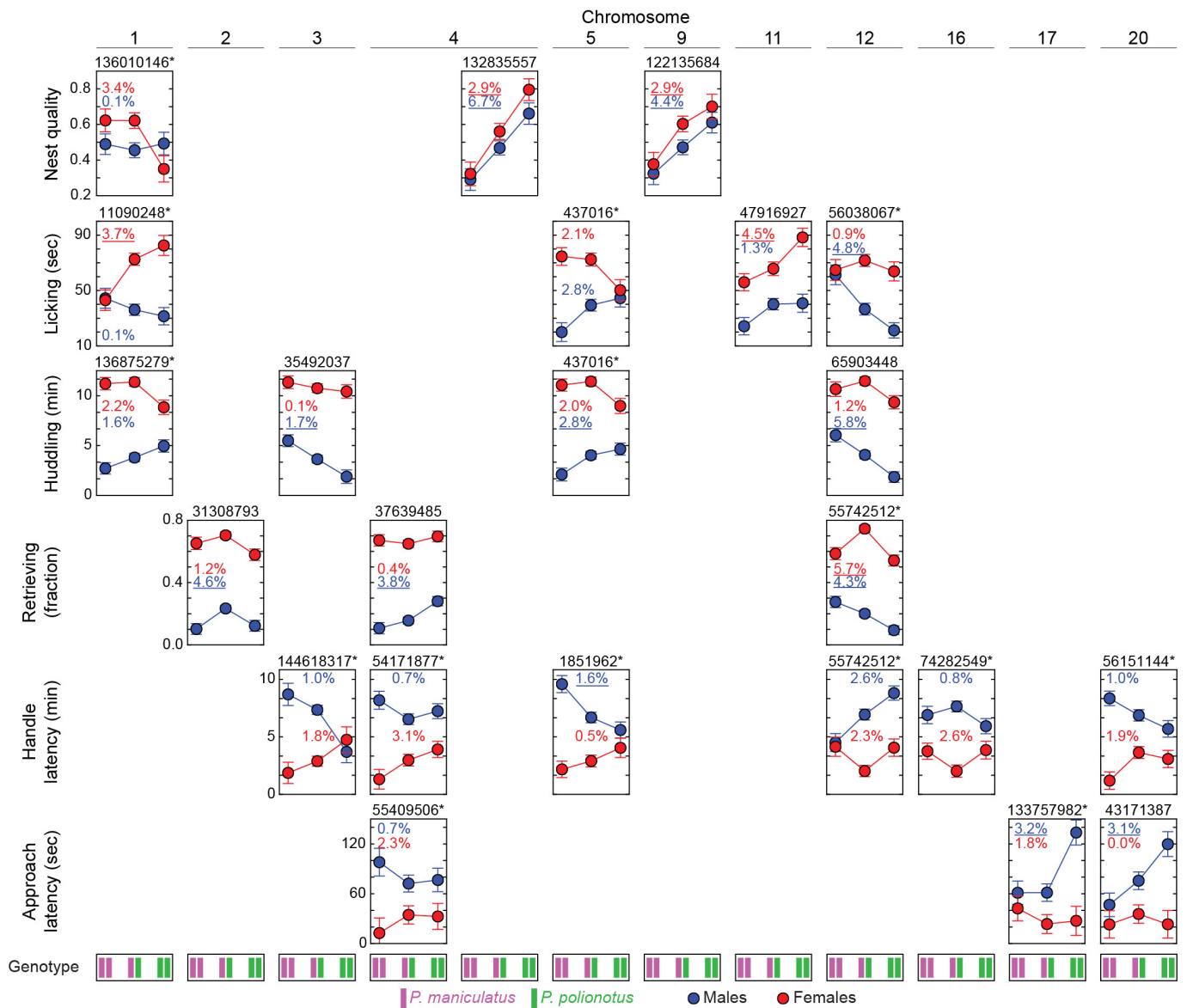
Extended Data Figure 2 | Parental behaviours towards own pups and heterospecific pups. The behaviour of parents was measured across 4 consecutive days, alternating the pup species each day (randomizing the pup that was given on day 1). Grey lines connect an individual's behaviour. Blue and red lines denote the median for fathers and mothers, respectively. * $P < 0.05$; ** $P < 0.01$; NS, not significant by paired t -test or Wilcoxon signed-rank test (nest quality).



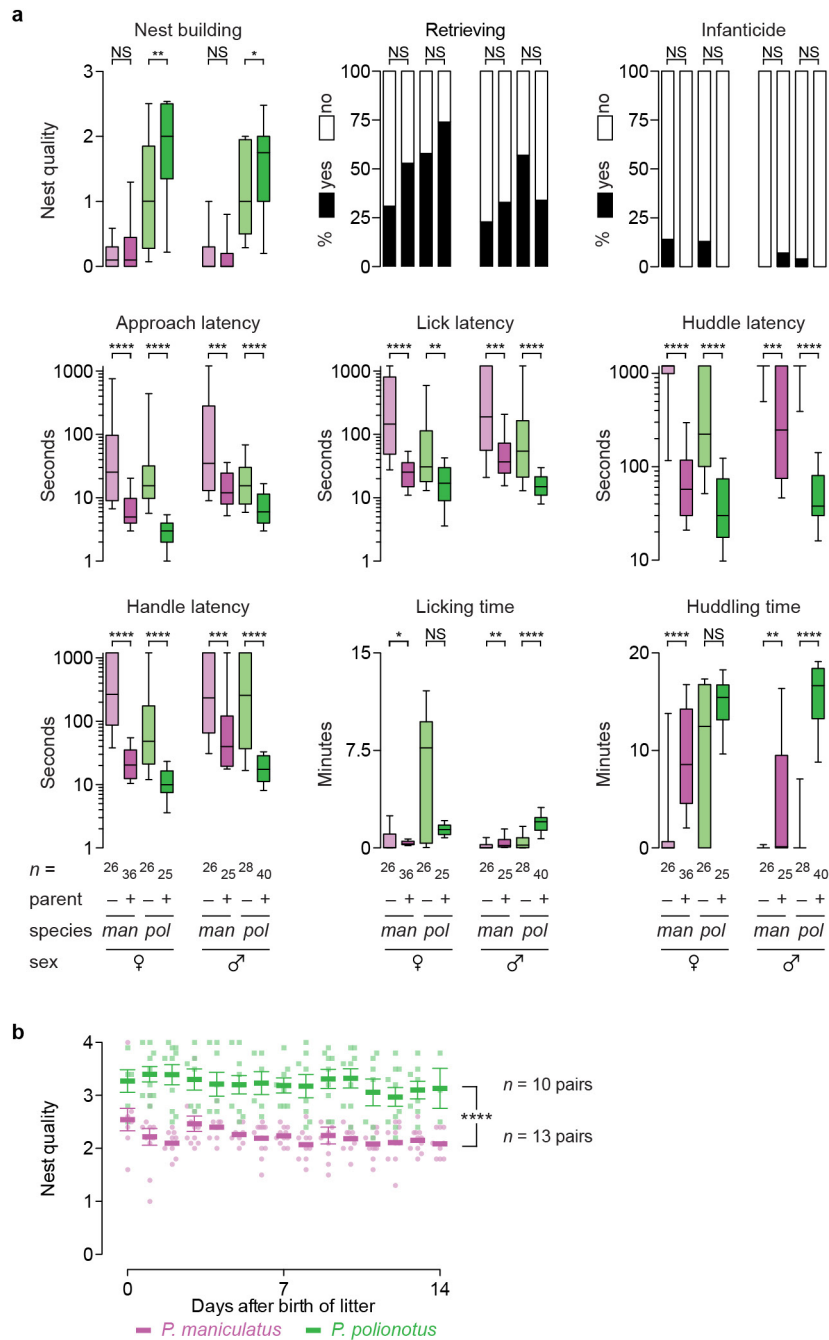
Extended Data Figure 3 | QTL mapping of parental behaviours.

Non-parametric interval mapping of (a) six parental behaviours in males ($n = 419$) and females ($n = 350$), and (b) the subset of F_2 animals that performed a behaviour (that is, excluding the animals that did not huddle or lick their pups for the duration of all three trials). Sample sizes for huddling were as follows: males, 259; females, 300; for licking: males, 319; females, 313. c, Haley-Knott regression on nqrnk normalized values of all F_2 individuals, using sex as a covariate. Plots show the difference in lod

scores for the scan with sex as an interactive and as an additive covariate minus the scan with sex as an additive covariate alone. The artificial narrow peaks at the ends of chromosomes result from lack of genotype imputation by MSG at chromosome ends (nest quality, chromosome 22; latency to approach, chromosome 9; latency to handle, chromosome 14). a–c, Dashed lines denote the $P = 0.05$ genome-wide significance level determined by 1,000 permutations.

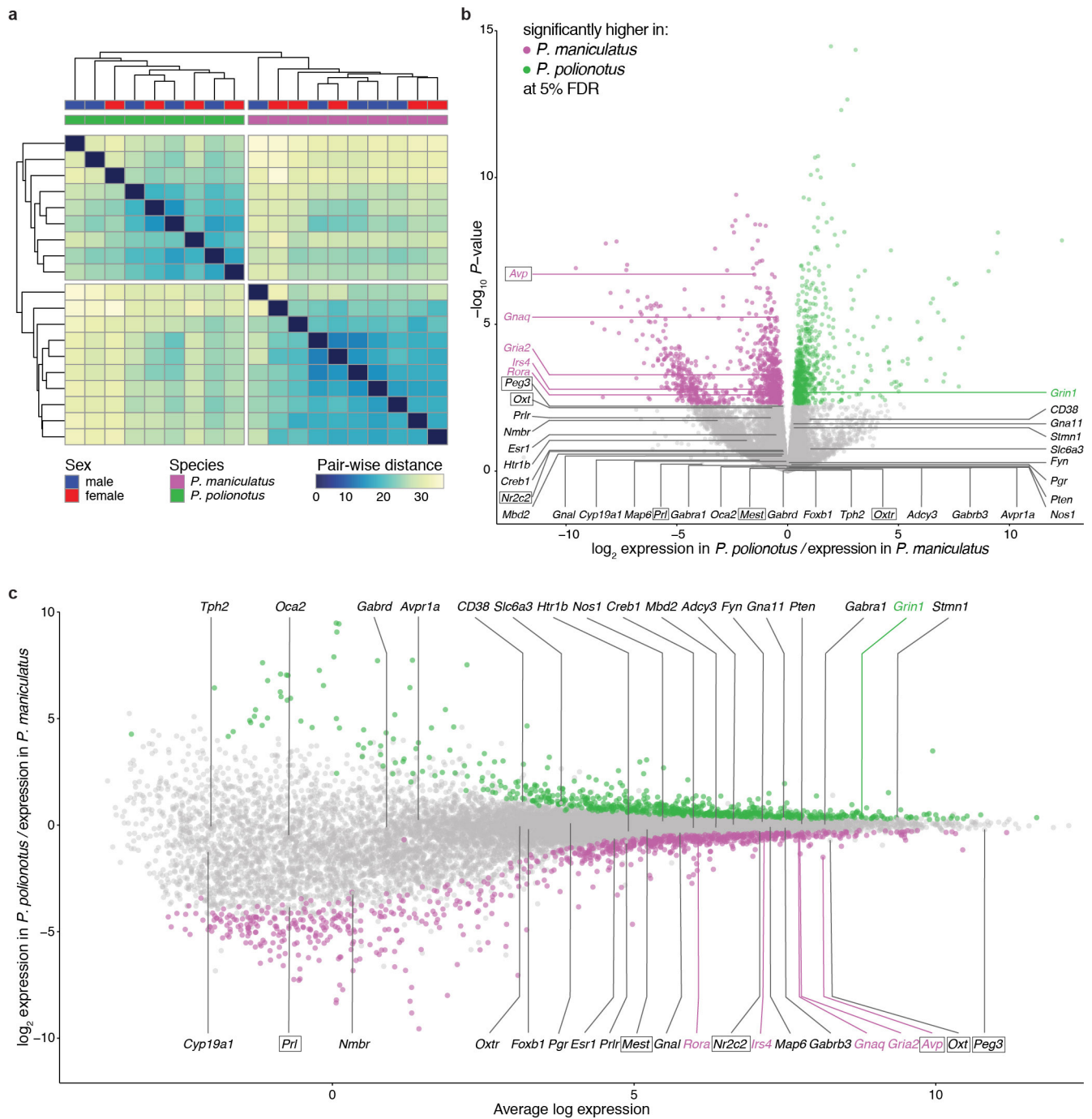


Extended Data Figure 4 | QTL effect plots. Phenotype means (\pm s.e.m.) against genotypes at peak QTL markers reported in Fig. 4 and Extended Data Fig. 3. Above each graph is the chromosomal position of the QTL peak. *Significant QTL-by-sex interaction. The per cent variance explained is given for each QTL and is underlined if the QTL was significant in a QTL analysis of that sex (Extended Data Fig. 3a, b).



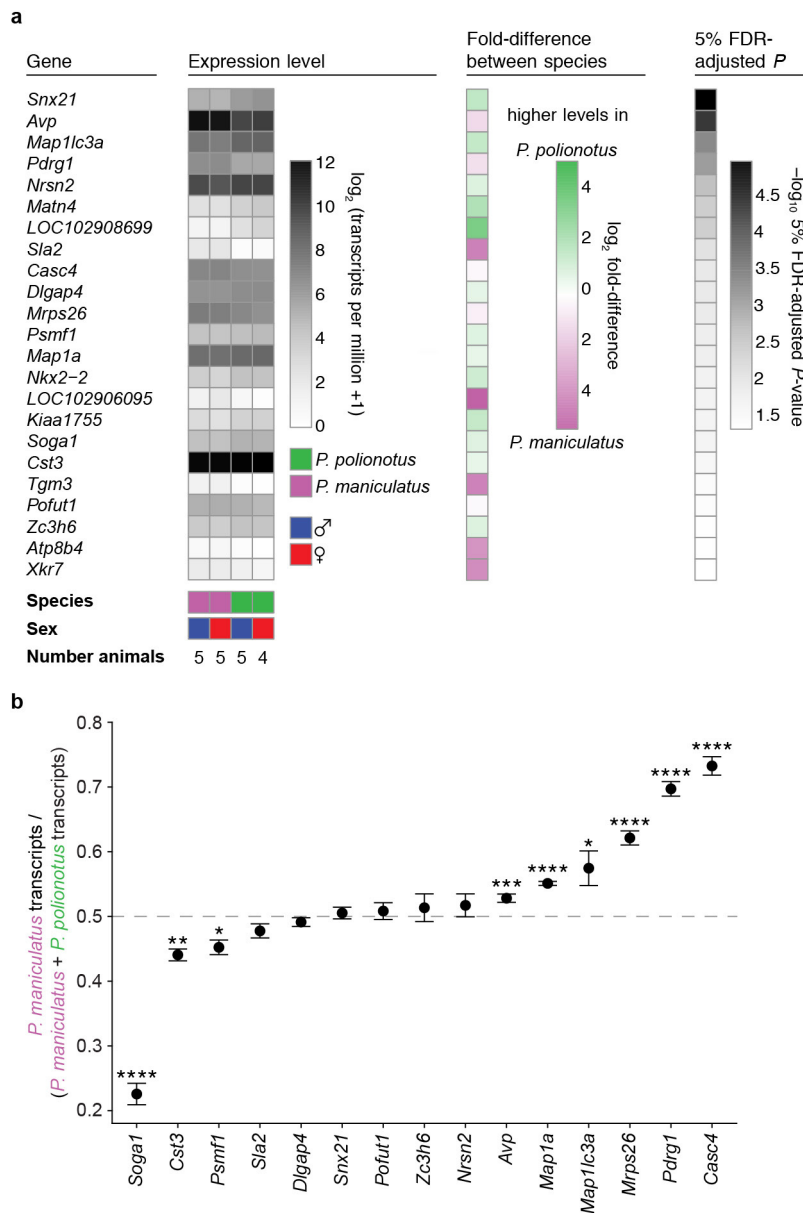
Extended Data Figure 5 | Behaviour of sexually naive and parental animals. a, Sexually naive animals were tested with 4- to 6-day-old conspecific pups, and parents with their own 4- to 6-day-old pups. Box plots indicate median, interquartile range, and 10th–90th percentiles. *P. maniculatus* (*man*, magenta) and *P. polionotus* (*pol*, green). * $P < 0.05$; ** $P < 0.01$; *** $P < 0.001$; **** $P < 0.0001$; NS, not significant by Mann–Whitney *U*-test or Fisher’s exact test (retrieving and infanticide). **b,** Nest quality (mean \pm s.e.m., and each pair in magenta circles for

P. maniculatus and green squares for *P. polionotus*) in the 2 weeks after the birth of a litter. Existing nests were removed from the parents’ cage at the time of weaning and 5 g of new cotton nesting material (Nestlet) was provided. Litters were born 1–4 days after weaning the previous litter, and nest quality was evaluated once a day in the home cage, where both mother and father were present. **** $P < 0.0001$ effect of species in a two-way ANOVA including species and time as factors. There was no significant effect of time or species-by-time interaction.



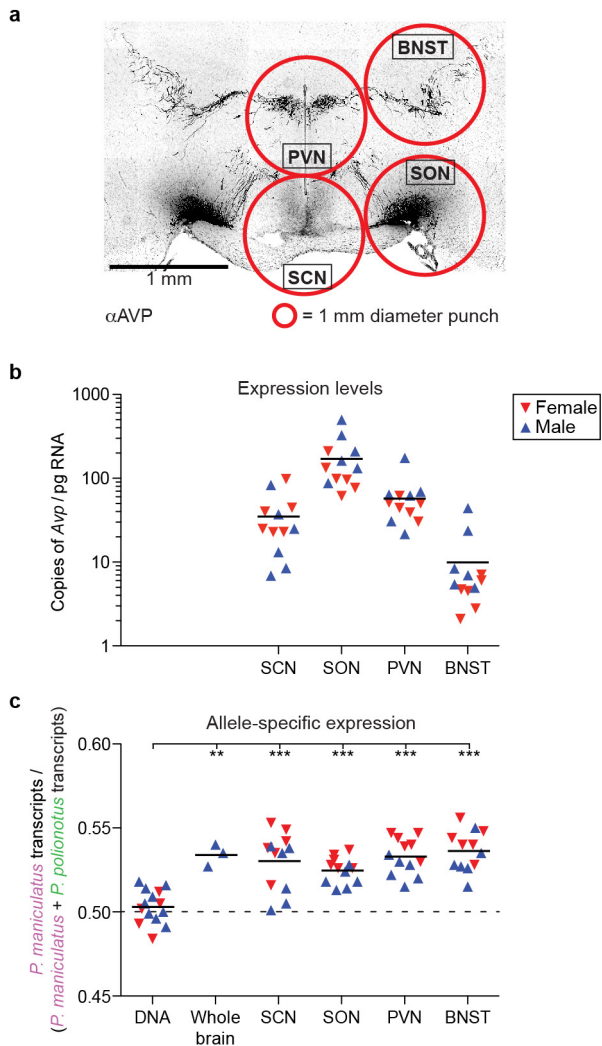
Extended Data Figure 6 | RNA-seq analysis of *P. maniculatus* and *P. polionotus* hypothalamus. **a**, Clustering dendrogram of RNA-seq samples by Euclidian distances of transcript expression levels. Samples cluster by species but not by sex. **b**, Strength of differential expression between species. Each circle represents a gene and is colour-coded in magenta or green if its differential expression was significant at a

5% FDR. **c**, Relationship between average gene expression level and differential expression between species. In both **b** and **c**, genes that have been associated with parental care in previous studies (by physiological/pharmacological studies or induced mutations)^{64–66} are labelled; the gene is also boxed if located inside parental behaviour QTLs identified in this study.

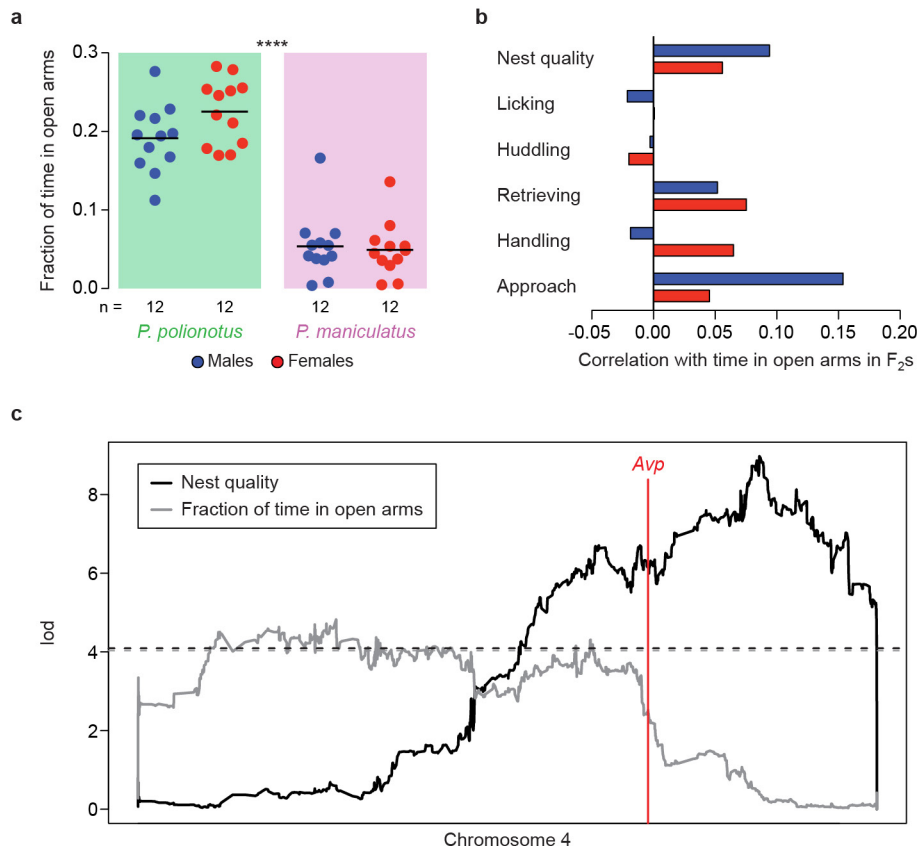


Extended Data Figure 7 | Expression analysis of genes in the chromosome 4 nest-building QTL. a, Twenty-three genes that are differentially expressed in the hypothalamus at 5% FDR between *P. maniculatus* and *P. polionotus*, sorted by FDR-adjusted *P* value. There were no significant differences between sexes for any gene. For each gene, its average expression level in each species and sex is shown on the left, the fold-difference in expression between the species in the middle, and the FDR-adjusted *P* value on the right. **b,** Allele-specific expression of the

15 genes from **a** for which interspecific genetic variation allows this analysis. Mean fraction of reads (\pm s.e.m.) matching the *P. maniculatus* allele from RNA-seq of the hypothalamus of 12 male and 12 female *P. maniculatus* \times *P. polionotus* F₁ hybrids. There were no significant differences between males and females, so the sexes were combined for the plot. **P* < 0.05; ***P* < 0.01; ****P* < 0.001; *****P* < 0.0001 by a linear model measuring allelic bias for each gene: $\ln(\text{allelic bias}) = \alpha + \beta \times \text{sex} + \epsilon$.

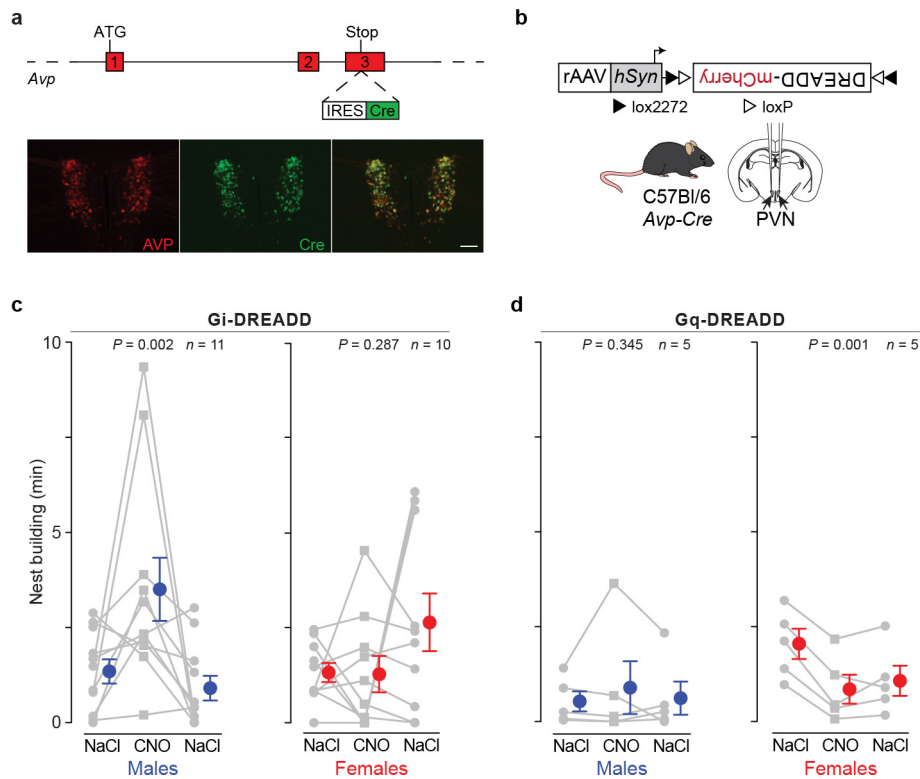


Extended Data Figure 8 | Allele-specific expression of *Avp* in different brain regions. **a**, Immunofluorescence staining of vasopressin in a coronal section of a *P. maniculatus* male brain, showing the main vasopressin-producing nuclei. Red circles illustrate the 1 mm diameter (1.5 mm thick) circular punches used to microdissect these nuclei. **b**, **c**, Number of *Avp* transcripts (**b**) and allele-specific expression of *Avp* (**c**) in each of the microdissected regions in *P. maniculatus* × *P. polionotus* F₁ hybrid animals, measured by droplet-digital PCR; horizontal line at the mean. ** $P < 0.01$; *** $P < 0.001$ by ANOVA with Bonferroni correction. SCN, suprachiasmatic nucleus; SON, supraoptic nucleus; PVN, paraventricular nucleus of the hypothalamus; BNST, bed nucleus of the stria terminalis.



Extended Data Figure 9 | Relationship between anxiety and nest building. **a**, Fraction of time in the open arms of an elevated plus maze. Line at the mean. **** $P < 0.0001$ for difference between species by two-way ANOVA with sex and species as factors. No significant effect of sex or sex-by-species interaction. **b**, Spearman's correlation coefficients among F_2 mice between fraction of time in the open arms and parental behaviours. Handling and approach are promptness to perform those

behaviours. **c**, Linkage (lod score) to chromosome 4 of nest-building behaviour and fraction of time in open arms. Males and females combined since there are no major differences in the lod scores between sexes. Red line denotes the location of *Avp*. Dashed lines denote the $P = 0.05$ genome-wide significance level determined by 1,000 permutations of each trait ($n = 769$).



Extended Data Figure 10 | Chemogenetic experiments on vasopressin neurons of *M. musculus*. **a**, Generation of *Avp-Cre* BAC-transgenic *M. musculus*. Top: schematic diagram illustrating the targeting of the IRES-Cre cassette immediately after the *Avp* stop codon. Bottom: immunofluorescence histology of vasopressin (AVP) and Cre in the paraventricular nuclei (PVN) of the hypothalamus of an *Avp-Cre* BAC-transgenic *M. musculus*. Scale bar, 100 μ m. **b**, A recombinant adeno-associated virus (rAAV) containing a Cre-dependent DREADD was

injected into the PVN of *Avp-Cre* transgenic *M. musculus*. **c**, **d**, Nest-building behaviour for 1 h after intraperitoneal injection with 0.9% NaCl or with the DREADD agonist clozapine-*N*-oxide (CNO) at 10 mg per kg. In **c**, animals expressed the inhibitory Gi-DREADD and in **d**, the excitatory Gq-DREADD. Males (with blue symbols at the mean \pm s.e.m.) are on the left and females (red) are on the right in each panel. Statistical significance determined by repeated-measures ANOVA for quadratic trend.